National Library of Canada
Acquisitions and Bibliographic Services Branch
395 Wellington Street
Ottawa, Ontario
K1A 0N4

Bibliothèque nationale du Canada
Direction des acquisitions et des services bibliographiques
395, rue Wellington
Ottawa (Ontario)
K1A 0N4

Your file Votre référence

Our file Notre référence

NOTICE

The quality of this microform is heavily dependent upon the quality of the original thesis submitted for microfilming. Every effort has been made to ensure the highest quality of reproduction possible.

If pages are missing, contact the university which granted the degree.

Some pages may have indistinct print especially if the original pages were typed with a poor typewriter ribbon or if the university sent us an inferior photocopy.

Reproduction in full or in part of this microform is governed by the Canadian Copyright Act, R.S.C. 1970, c. C-30, and subsequent amendments.

AVIS

La qualité de cette microforme dépend grandement de la qualité de la thèse soumise au microfilmage. Nous avons tout fait pour assurer une qualité supérieure de reproduction.

S'il manque des pages, veuillez communiquer avec l'université qui a conféré le grade.

La qualité d'impression de certaines pages peut laisser à désirer, surtout si les pages originales ont été dactylographiées à l'aide d'un ruban usé ou si l'université nous a fait parvenir une photocopie de qualité inférieure.

La reproduction, même partielle, de cette microforme est soumise à la Loi canadienne sur le droit d'auteur, SRC 1970, c. C-30, et ses amendements subséquents.

Canada

UNIVERSITY OF ALBERTA

OPTICAL PROPERTIES OF WOOD

BY

DAMMIKA VITHANA

©

A THESIS

SUBMITTED TO THE FACULTY OF GRADUATE STUDIES AND RESEARCH IN

PARTIAL FULFILMENT OF THE REQUIREMENTS FOR THE DEGREE OF

MASTER OF SCIENCE

DEPARTMENT OF PHYSICS

EDMONTON, ALBERTA

FALL 1994

National Library
of Canada

Acquisitions and
Bibliographic Services Branch

395 Wellington Street
Ottawa, Ontario
K1A 0N4

Bibliothèque nationale
du Canada

Direction des acquisitions et
des services bibliographiques

395, rue Wellington
Ottawa (Ontario)
K1A 0N4

Your file Votre référence

Our file Notre référence

The author has granted an irrevocable non-exclusive licence allowing the National Library of Canada to reproduce, loan, distribute or sell copies of his/her thesis by any means and in any form or format, making this thesis available to interested persons.

L'auteur a accordé une licence irrévocable et non exclusive permettant à la Bibliothèque nationale du Canada de reproduire, prêter, distribuer ou vendre des copies de sa thèse de quelque manière et sous quelque forme que ce soit pour mettre des exemplaires de cette thèse à la disposition des personnes intéressées.

The author retains ownership of the copyright in his/her thesis. Neither the thesis nor substantial extracts from it may be printed or otherwise reproduced without his/her permission.

L'auteur conserve la propriété du droit d'auteur qui protège sa thèse. Ni la thèse ni des extraits substantiels de celle-ci ne doivent être imprimés ou autrement reproduits sans son autorisation.

ISBN 0-315-95127-3

Canada

UNIVERSITY OF ALBERTA

RELEASE FORM

NAME OF AUTHOR : DAMMIKA VITHANA

TITLE OF THESIS : OPTICAL PROPERTIES OF WOOD

DEGREE : MASTER OF SCIENCE

YEAR THIS DEGREE GRANTED : 1994

Permission is hereby granted to the University of Alberta Library to reproduce single copies of this thesis and to lend or sell such copies for private, scholarly or scientific research purposes only. The author reserves all other publication and other rights in association with the copyright in the thesis, and expect as hereinbefore provided neither the thesis nor any substantial portion thereof may be printed or otherwise reproduced in any material form whatever without the author's prior written permission.

(Student's Signature)

"Sumaga"
Miltzananda Estate
Matara, Sri Lanka

(Student's Permanent Address)

Date: August 31, 1994.

UNIVERSITY OF ALBERTA

FACULTY OF GRADUATE STUDIES AND RESEARCH

The undersigned certify that they have read, and recommended to the Faculty of Graduate Studies and Research for acceptance, a thesis entitled **OPTICAL PROPERTIES OF WOOD** submitted by DAMMIKA VITHANA in partial fulfilment of the requirements for the degree of MASTER OF SCIENCE.

Supervisor

External Examiner

Date: Aug 30 '94

DEDICATION

TO MY PARENTS AND TEACHERS

ABSTRACT

This thesis is an attempt made by us to distinguish discolored wood from sound wood and to identify characteristics of defects by measuring optical properties of the wood. The work is concentrated on aspen wood which is a major raw material for paper production in Canada.

One of the largest concerns affecting the utilization of aspen is the presence of wood decay and stain which result in discoloration or reduction of strength. Decayed wood causes problems in pulping and bleaching in the manufacture of paper. Ideally it should be separated from the sound wood before it enters the pulping system. An automated recognition system of clear wood from seriously defective wood will be of great advantage in the industry.

The samples examined were cross-sectional slices of aspen wood, each approximately 3 cm thick, through trunks of different aspen trees.

Reflection intensities of the wood slices were measured with reference to the standard which is the clearest among the samples. The wavelength region investigated was 390 to 1100 nm. Higher reflection intensities were obtained for lighter samples than darker samples. Although the reflection intensities of brown and clear wood samples with respect to the clear aspen wood decrease with decreasing wavelength, there is again an increase in the violet and near UV region with a minimum around $\lambda = 450$ nm. For a sample which has black patches, a significant difference can be seen in reflection intensities with

respect to the clear wood because its reflection intensity continuously increases with decreasing wavelength. The best region where the brown wood can be distinguished from the clear wood is the blue region in the spectrum.

Light transmission through thin wood samples, which were taken from the large slices, was also measured. As in reflection measurements, the wavelength region investigated was 390 to 1100 nm. Higher relative transmission intensities are obtained for the clear wood than stained wood. It was also seen that there are striking differences in transmission for both clear and stained wood when the light enters along the grain as compared to entering across the grain. Light travelling along the grain is attenuated much less than light travelling across the grain. Absorption coefficients were calculated and plotted against wavelengths. Higher absorption coefficients are found for light travelling across the grain than light travelling along the grain for both clear and discolored wood samples.

Photoluminescence response of discolored aspen wood slices was detected in the wave length range of 500 to 620 nm with a peak at 535 nm. It was noted that only the edges of the certain types of discolored parts give luminescence. The shape of photoluminescence spectrum does not depend on the type of the disease. An attempt was made to measure decay times at room temperature and liquid nitrogen temperature but the response times of the order of 1 ns were too short to be resolved.

ACKNOWLEDGEMENT

I would like to acknowledge my indebtedness to all who have helped me in this undertaking, Dr. F. L. Weichman, my supervisor, Ken Marsh and Bill Burris, technicians of the Physics Department, Dr. Y. Hiratsuka of the Forestry Canada, and Visionsmart Inc. for providing samples. I am most greatful to these individuals for their efforts and encouragement extended to me.

Table of Contents

Chapter		page
1	Introduction	1
	1.1 Objective of the thesis	1
	1.2 Aspen Wood Resource	1
	1.3 Characteristics, Structure and Composition	2
	1.31 Macroscopic Characteristics	2
	1.32 Physical Characteristics	2
	1.33 Microscopic Characteristics	3
	1.34 Composition of Wood	4
	1.341 Elementary Chemical Composition	4
	1.342 Organic Components	4
	1.4 Wood Chemistry of Aspen	5
	1.5 Decay and Stain	6
	1.51 Categories of Wood Defects	6
	1.511 Traditional Classification System	6
	1.512 New classification system	7
	1.6 Background and Objectives	9
	1.7 Samples	9
2	Reflection Measurements	15
	2.1 Background	15
	2.2 Equipment and Procedure	15
	2.3 Samples	20
	2.4 Results and Discussion	22

3 Transmission Measurements 31

3.1 Background 31

3.2 Equipment and Procedure 31

3.3 sample Preparation 34

3.4 Results and discussion 34

3.5 Transmission Analysis 40

3.51 Assumptions 40

3.52 Calculations 41

3.53 Results and Discussion 44

4 Luminescence Spectroscopy 51

4.1 Background 51

4.2 Equipment and Procedure 51

4.3 Samples 54

4.4 Results and discussion 54

4.41 Luminescence intensity 54

4.42 Life Time 55

5 Summary and Discussion 61

Bibliography 67

Appendix I 71

List of Figures

		page
1.	The distribution of aspen trees across Canada.	10
2.	Chemical composition of aspen wood.	11
3.	Experimental setup for reflection measurements.	16
4.	Schematic diagram of Kipp & Zonen mirror double monochromator.	17
5.	Relative response vs wavelength of a S-1 photomultiplier tube.	18
6.	Schematic diagram of sample holder and assembly for reflection measurements.	21
7.	Relative reflection vs wavelength for W-4 (vs ceramic).	26
8.	Relative reflection vs wavelength for W-3.	27
9.	Relative reflection vs wavelength for W-5.	28
10.	Relative reflection vs wavelength for W-8.	29
11.	Relative reflection vs wavelength for W-9.	30
12.	Experimental setup for transmission measurements.	32
13.	Schematic diagram of sample holder and assembly for transmission measurements.	33
14.	Relative transmission vs wavelength of w-9 (clear wood, light along the grain).	35
15.	Relative transmission vs wavelength of w-9 (clear wood, light across the grain).	36
16.	Relative transmission vs wavelength of w-9 (discolored wood, light along the grain).	37

17. Relative transmission vs wavelength of w-9 (discolored wood, light across the grain). 38
18. Absorption coefficient vs wavelength for w-9. 39
19. Alignment of fibers in a tree. 42
20. Light paths in an isotropic, transparent cylindrical rod. 46
21. Decrease of energy for two arbitrary incident light rays per unit area with respect to the angle of incidence. 47
22. Relative transmission vs angle measured with respect to the incident light. 48
23. Relative transmission of five reflections vs angle measured with respect to the incident light. 49
24. Relative total transmission vs angle measured with respect to the incident light. 50
25. Experimental setup for luminescence measurements. 53
26. Relative luminescence intensity vs wavelength. 56
27. Decay curve (w-3, room temperature). 57
28. Decay curve (w-3, liquid nitrogen temperature). 58
29. Decay curve (w-7, room temperature). 59
30. Decay curve (w-7, liquid nitrogen temperature). 60

List of Tables

		page
1.	Chemical composition of several common wood species.	5
2.	Details of the defect categories of aspen wood .	12
3.	Brief description of the wood slices studied.	13
4.	List of samples identified for the category of defects.	14

CHAPTER 1

Introduction

1.1 Objective of the Thesis

The idea for this thesis arose out of a request of Visionsmart Inc. to measure light reflections of aspen wood to search for useful identifiable characteristics between sound wood and defective wood that could eventually lead to automated defect recognition in the pulp and paper industry. The study was then expanded to other optical properties such as transmission and luminescence as a general interest study of easily measurable optical properties of aspen wood. Some of the variables that were controlled were wavelength, thickness of the wood sample, and the grain direction of the wood.

1.2 Aspen Wood Resource

In volume of standing timber, Canada's aspen resource is very large: about 2.2 billion cubic meters. That is more than twice the volume of birch, number two in the hardwood family, and almost five times the volume of maples. Figure 1 illustrates the widespread distribution of aspen across Canada. Aspen represents about three-quarters of the country's stock of poplars. Aspen growth is particularly dense in a wide diagonal band from Northeastern British Colombia to Northern Ontario. Alberta has 30% of Canada's total aspen resource. The total volume of aspen in the province of Alberta is approximately 850 million m^3. Alberta's aspen stock is approximately equal to that of the entire United States (Macleod,1987).

1.3 Characteristics, Structure and composition of Wood

1.31 Macroscopic Characteristics

Macroscopic characteristics are those features visible with naked eye, or with a hand lens capable of magnifying 10-15 times. The macroscopic appearance of wood varies according to the plane at which it is sectioned and viewed - in relation to the longitudinal axis of a tree.

Wood is characterized by the presence of more or less conspicuous concentric layers, known as growth rings or annual rings. This pattern is due to the mechanism of tree growth, which takes place by super-position of structurally different layers. In temperate zones there is, as a rule, one such wood layer added during each season of growth. Although in most species, growth rings can be easily distinguished, in aspen and other trees of the poplar family, growth rings are more difficult to see.

Wood is divided into two groups: hardwood and softwood. Needle-like leaves which remain green the year around characterize softwoods. In contrast to softwoods, hardwoods have broad leaves which generally drop in the fall. Aspen is a hardwood in the poplar family.

1.32 Physical characteristics

In addition to the macroscopic characteristics, there are a number of other physical characteristics, such as color, luster, odor, taste, texture, grain, figure, weight, and hardness.

Wood comes in a variety of natural colors which may range from almost white to

jet black. Although healthy aspen wood is exceptionally white in color, the decay due to fungal attack changes its color to brown and even black.

The grain denotes direction of wood elements. When the grain changes; ie. the direction of the wood cells changes, we can expect differences in optical properties of wood. It was, therefore, important to while measuring reflection and transmission to keep the grain direction as a variable.

1.33 Microscopic Characteristics

Wood is composed of a multitude of minute units, called cells. Cells of softwood species differ in appearance from cells of hardwood species. Although both hardwoods and softwoods are composed of tube-like cells, the ends of the cells are different and there is a variation in size . The ends of the cells of hardwoods are closed and pointed while softwoods cells have closed and blunt ends. These cells are called fibers. In addition, what we call a piece of wood contains other type of cells called vessel members and parenchyma cells which are shorter and wider than the fibers. The thickness of walls of fibers varies depending on the species. Length of the fibers also varies between species, ranging on the average between 1 and 2 mm (exceptionally 0.5 - 2.5 mm). Diameters range from about 0.01 to 0.05 mm.

1.34 Composition

1.341 Elementary Chemical Composition

With regard to elementary chemical composition there are no important differences among woods. The principal chemical elements of wood are carbon (C), hydrogen (H), and oxygen (O); small amounts of nitrogen (N) are also present. In addition to the above, there are small amounts of mineral elements such as calcium (Ca), potassium (K), and magnesium (Mg).

1.342 Organic Components

Carbon, hydrogen, and oxygen combine to form the principal organic components of wood substance, namely cellulose, hemicelluloses, and lignin. These organic components of wood are not simple chemical entities that can be identified. The terms (cellulose, hemicelluloses, etc.) are generic, and each includes a number of chemically related compounds.

Cellulose, a high molecular weight polymer, which appears in the wood cells, is synthesized directly from units of glucose. Glucose molecules are linked together to form long cellulose chain molecules.

Hemicellulose, a relatively low molecular weight polymer , which also appears in the wood cells, is synthesized from other sugars (eg. glactose) along with glucose. Both cellulose and hemicellulose are carbohydrates.

Lignin is a polymer complex and high molecular weight polymer composed of carbon, nitrogen, and oxygen. Lignin occurs between individual cells and within the cell walls. Between cells, it serves as a binding agent to hold the cells together. Within cell walls lignin is intimately associated with cellulose and serves to impart rigidity to the cell.

1.4 Wood chemistry of Aspen

Unusual wood chemistry is the feature which distinguishes aspen from all the other important wood species in Canada. Figure 2 shows that in general terms, cellulose accounts for more than 50% of aspen wood, while the lignin content is typically 20% or less. Total hemicellulose content is about 30%. The corresponding values of several other common wood species are listed in Table 1, from which it is apparent that, in chemical terms, aspen is unique.

Table 1

	Cellulose	Lignin	Hemicellulose
Trembling Aspen	53	16	31
Red maple	44	24	32
Balsam Fir	45	29	26
Jack Pine	42	29	29
White Spruce	45	27	28

Two simple consequences stem from aspen's chemical composition. First, the low lignin content. Low lignin content means that aspen wood can be softened or delignified more easily than any of the other wood species in Table 1. Thus chemical pulping can be fast and efficient. Second, the high cellulose content in the wood leads to comparatively high pulp yields from chemical processes. These things go hand-in- hand.

It is also true that sound, fresh aspen wood is an exceptionally "white" wood; as a consequence, pulps made from it are relatively light in color even before any chemical bleaching or brightening is done. But it is very important to note that biological decay and stain can greatly reduce the brightness of the wood and therefore that of the pulp.

1.5 Decay and Stain

Large numbers of species of fungi are known to cause or to be associated with the decay in aspen (Lindsey and Gilbertson 1978). Most are decay fungi of standing dead or fallen trees and are minor importance to live aspen. Seventeen species of fungi have been identified which cause decay of standing live aspen (Thomas et al. 1960).

1.51 Categories of wood defects

1.511 Traditional classification

A widely used traditional classification system categorizes wood defects as incipient decay, advanced decay, and stain. In incipient decay fungi eat up all the lignin in fiber wall and leave cellulose behind. Therefore, within the pulp and

paper industry, incipient decay does not do any harm. After the initial attack of incipient decay where the fungus has just entered the fiber, and has eaten part of the lignin and some of other sugars, the cellulose structure itself is now attacked. Therefore two effects occur: one is the reduction of material; and the second, a degradation or reduction of the intrinsic strength of the fiber. This traditional classification has created problems in judging and recording wood defects in aspen. There is no clear agreement on the classification of decay and stain into these categories for the measurement processes of decay.

1.512 New Classification System

Five major categories of wood defects have been described in detail for the purpose of decay and stain measurements by Hiratsuka,Y, Gibbard, D. A. , Bakowsky, O., and Maier, G. B. (1990). The classification which is shown in Table 2 involves both visual characteristics and hardness of the wood.

i. Type A

This category is characterized by a prominent black line that surrounds and often occurs within decayed areas. The rot, caused by a fungus, is white, spongy, and soft. Most of the category of advanced decay of the traditional classification system was likely caused by this fungus. This defect is characterized by a long decay column, frequently continuing along most of the main stem, less frequently in the bottom part of the trunk. Extensive decay of this type usually occurs more than 2 m above the ground.

ii. Type B

The yellow, stringy rot is often covered by dark brown fungal material mixed with wood. Black shoestring - like fungal structures are often found within and around the decay. The Type B defect occurs only at the bottom of the tree and tapers off quickly, seldom extending more than 1 m above the ground.

iii. Type C

This category of defect is characterized by a general discoloration of the wood along with pockets of decay throughout the affected column. Decay and discoloration of wood classified as Type C are conspicuously pink to brownish pink and can occur along large columns of soft structural decay, and most of the affected wood stays relatively firm. Although hardness in general may not be reduced significantly, the infected wood may be more brittle than sound wood. Fibres of the affected areas often pull out, and cut surfaces have a rough appearance, while the adjacent sound wood cuts cleanly. A distinct splitting of wood often occurs between affected and healthy wood areas, causing a shrinkage and separation of annual rings. The Type C defect was recorded as incipient decay or stain under traditional classification system.

iv. Type D

All heartwood stains caused by fungi, bacteria, and non biotic factors which do not reduce wood hardness as in Types A, B, and C are categorized as Type D. Because Type D defects are caused by various biotic and abiotic agents, they are variable in distribution and extent.

v. Type E

This shows grayish and blackish sapwood stains that often develop in stored logs. These stains are caused by blue stain fungi. Type E stain typically develops from the log ends or damaged bark of the cut log.

1.6 Background and Objectives

If the decay is not particularly severe, it may cause only minor problems in pulping and bleaching. But, the more extensive the decay, the more severe the pulping problems: retarded delignification rates, lower pulp yields, darker pulp, more difficulty in bleaching, loss in pulp strength. Obviously the economic picture deteriorates as well. It is virtually impossible to harvest only the sound aspen trees, because the presence and extent of decay cannot be determined reliably in the standing trees. In fact, all the trees should be removed to facilitate regrowth. If the decay represents a large proportion of the wood mass, the decayed wood ideally should be separated from the sound wood before it enters the pulping system.

1.7 Samples

Ten cross-sectional slices, each approximately 3 cm thick, through trunks of different aspen trees, were given to us by Visionsmart Inc for testing, without specification of their defects. Table 3 gives a brief description of each slice as noted by an observer who is unfamiliar with aspen wood and its diseases. More recently, after we made our measurements, all ten samples were taken to Y. Hiratsuka (Forestry Canada) to identify the category of defects. Of all samples, only the four listed in Table 4 could be clearly categorized.

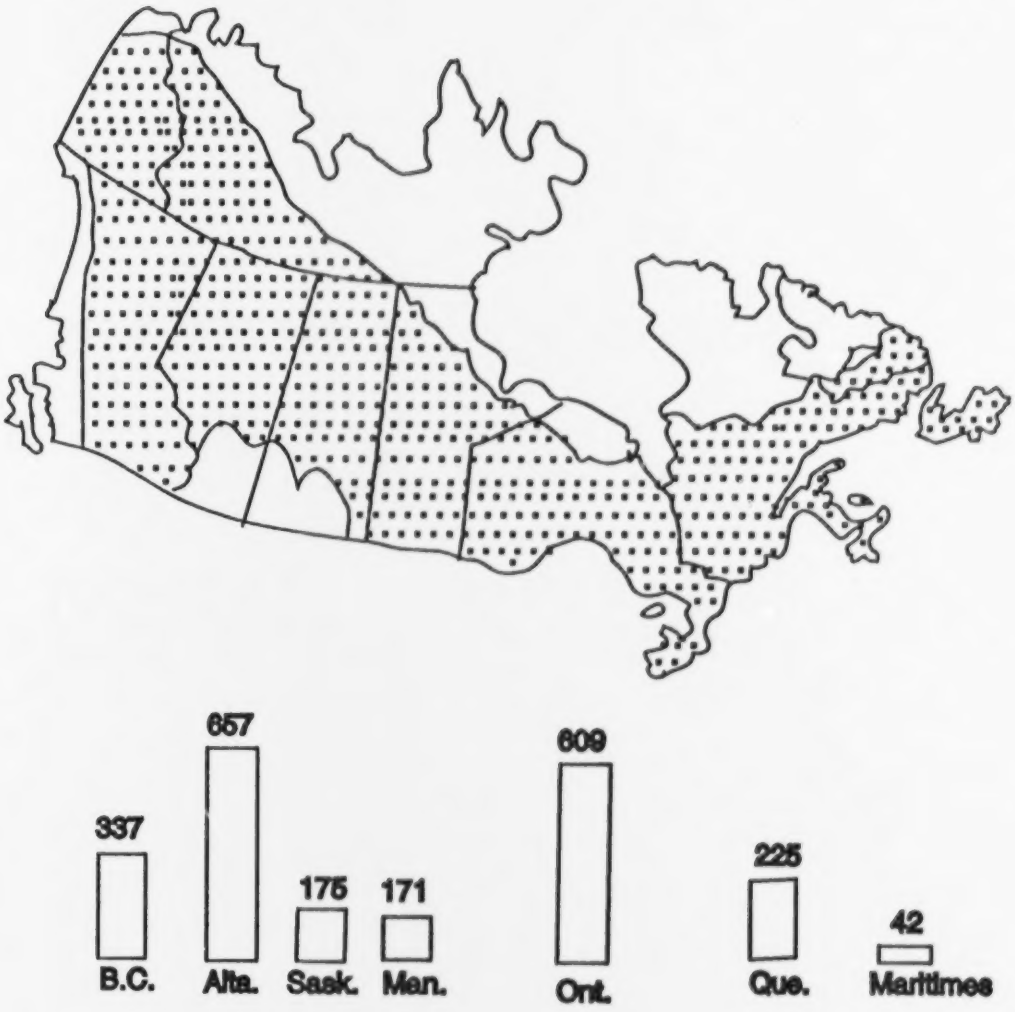

Figure 1

The distribution of aspen trees across Canada

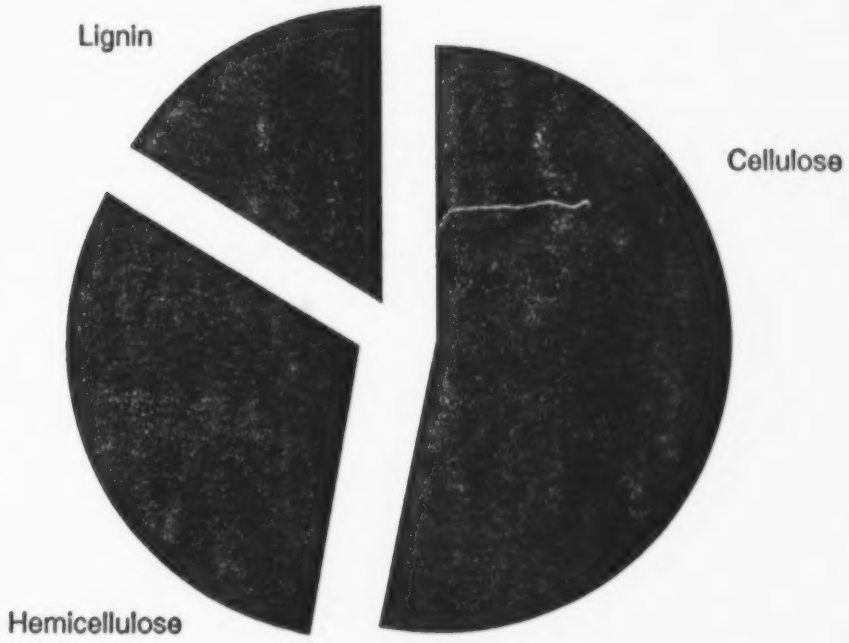

Figure 2

Chemical composition of aspen wood

Table 2

Type of defect	Causes	Description of defect and external indicators	Defect distribution
A	*Phellinus tremulae*	White spongy rot bordered with black lines. Usually associated with hoof-shaped conks.	Defects usually occur along most of the main stem, less frequently in the bottom part of the trunk.
B	mostly *Armillaria* species	Yellow, stringy rot often surrounded by dark brown fungal and wood material. Black shoestring-like fungal structures present in and around the decay.	Butt rot. Decay up to 1m above the ground.
C	Mostly *Peniophora polygonia*	stained column with irregular pockets of pinkish to brownish decay. Often associated with pink scale-like fruiting bodies.	Often occurs along large portions of the main stem.
D	Various causes (fungi, bacteria, nonbiotic factors)	Stain of various causes that does not reduce wood hardness.	Variable in distribution.
E	Blue stain fungi	Graish-black sapwood stain.	Occurs in sapwood. Initials from cut end or through damaged bark on stored logs.

Table 3

W-1	Slice of 2" thick, 6" diameter Rotten center is dusty: fibers no longer stick together
W-2	Slice of 2" thick, 6" diameter Old, dry wood with crack from the edge toward the center Brown spot in the very centre
W-3	Slice 2" thick, 9" diameter Dusty in the inner diameter portion Black figuring in more solid wood
W-4	Slice 2" thick, 5" diameter Small dark spot in the very center otherwise looks uniformly clear
W-5	Slice 2" thick, 6.5" diameter Fairly clean but has some greenish grey rings, 3.5" diameter
W-6	Slice 1.25" thick, 7" diameter Dusty region near center and a brown region from a rotten branch
W-7	Slice 2" thick, 6" diameter Some dusty sections, some light brown stain
W-8	Slice 2" thick, 6" diameter Combination of blemishes: green-grey and dark brown
W-9	Slice 2" thick and 10" diameter Deep crack from the bark inward Most of the area covered by large odd shaped stains
W-10	Generally looks clean

Table 4

Category of defects	Type A	Type C
Designation of the sample	W-9	W-5
	W-3	W-8

CHAPTER 2

Reflection Measurements

2.1 Background

The appearance and smoothness of the surfaces of the pure and discolored wood slices described in Table 3 are not the same. Since the reflection depends upon the color, the reflection characteristics of aspen wood were the starting point of the study.

2.2 Equipment and Procedure

Reflection intensities were measured using the experimental layout illustrated in figure 3.

A focused beam of white light enters through the slit of the monochromator. The beam is dispersed by the prism. Adjustment to the prism allows the operator to select a narrow wavelength range at the output slit. This selected light is passed on to either the sample or the reference after which the reflected light falls onto a phototube where its intensity is measured.

Light Source

A 55W (12V) quartz halogen automobile head lamp was used. (Model No: TUNGSRAM 50340). It is a bright source useful from the UV to near IR.

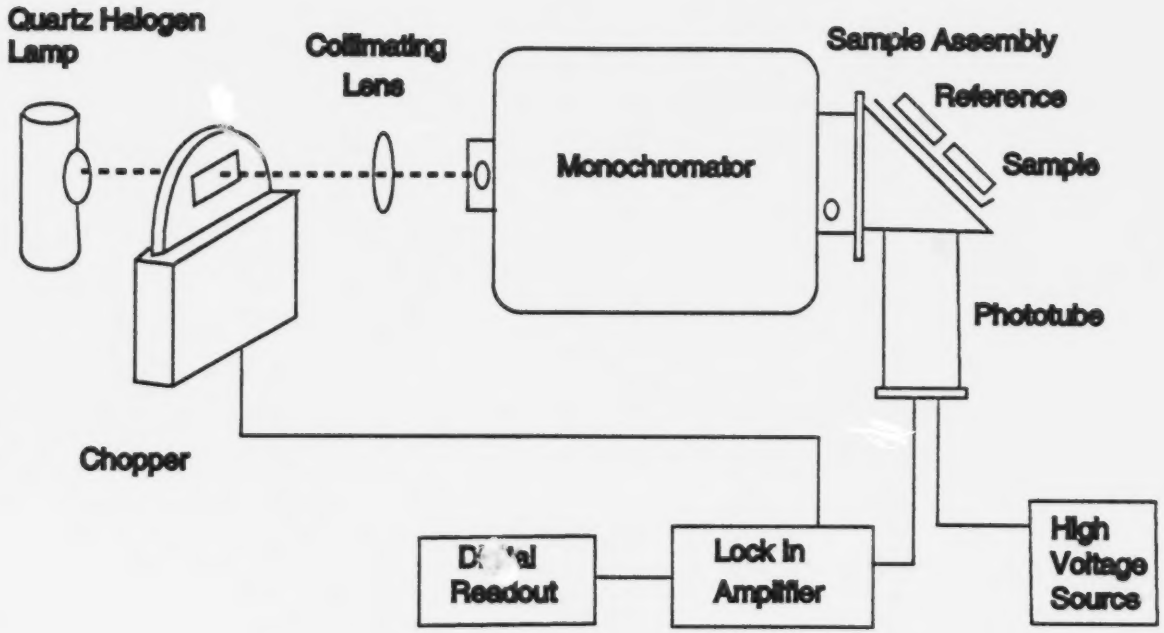

Figure 3 - Experimental setup for reflection measurements

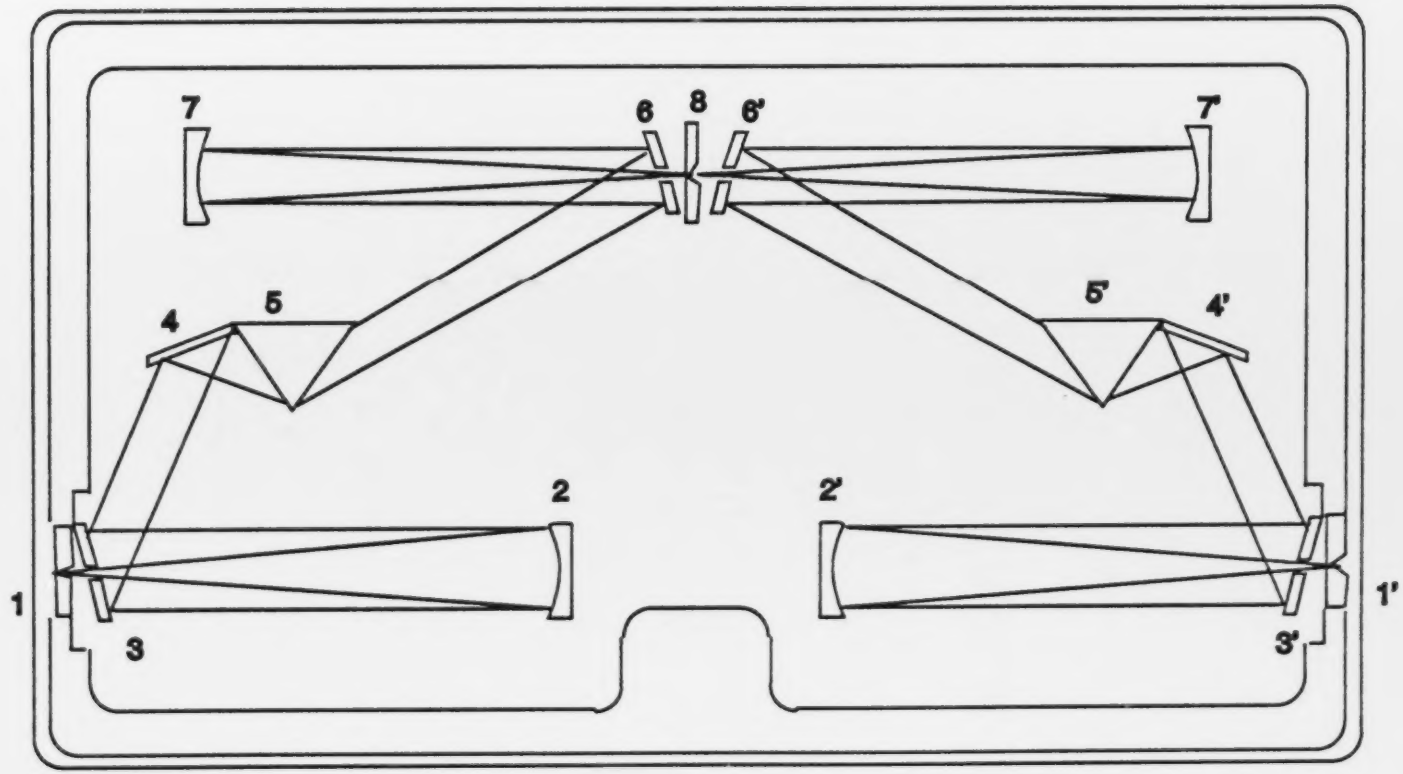

1,1' - bilateral slits 2,2',7,7' - concave mirrors 3,3',4,4',6,6' - plane mirrors 5,5' - prisms 8 - bilateral slit

Figure 4 - Schematic diagram of Kipp & Zonen mirror double monochromator

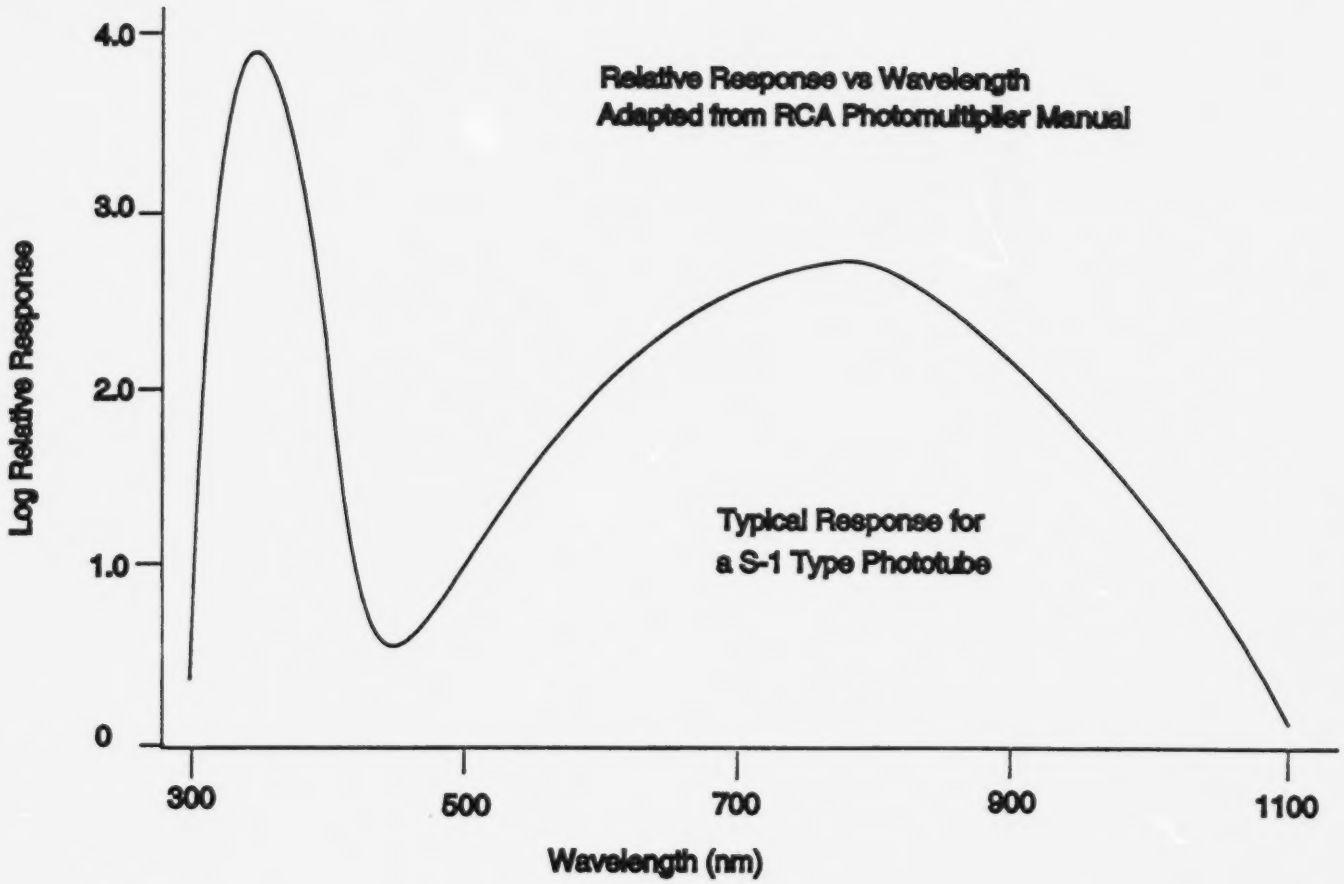

Figure 5 - Relative response vs wavelength of a S-1 photomultiplier tube

Monochromator

This mirror double monochromator-F/6 (Kipp & Zonen) uses two flint prisms (approximate refractive index 1.5, refractive angle 54°) to disperse the light. Figure 4 shows the internal optical arrangement.

A rotation of the prisms allows the selection of narrow wavelength intervals from the near ultra-violet to the near infrared region. Mirrors, instead of lenses, are used to eliminate chromatic aberration within the instrument.

Detector

The detector was a RCA 7102 S-1 response photomultiplier (PMT) working at 1200 volts delivered by a high voltage power supply (model PMT2N10KA, Spellman Highvoltage Electronics Corporation). The wavelength sensitivity of the PMT, although optimized for IR, limits the measurements to a maximum wavelength of 1.1μm. The typical response curve for a S-1 response tube is illustrated in figure 5.

Amplification and Noise Reduction System

The chopper was used to convert the constant intensity light source into one whose intensity alternates at a well defined frequency. The lock-in amplifier then only amplifies that part of the signal that has the correct fundamental frequency and phase as defined by the chopper.

Sample Holder and Assembly

The side view of the sample assembly and the sample holder are illustrated in figure 6. The quasi-monochromatic light from the exit slit was allowed to fall on a sample holder 35 mm away and inclined to the optical axis by 30°. The detector was mounted at right angles to the beam emerging from the exit slit, thus giving an angle of reflection of 60°, avoiding specular reflection angles. No lenses or mirrors were used between the exit slit and the detector.

The sample holder was a slider of aluminum with two identical round holes, 13 mm in diameter, large enough not to block any of the light from the exit slit. The wood sample was mounted against and behind one hole; the reference was mounted behind the other hole. The slider was constrained to move between accurately placed stops, allowing rapid and reproducible reflection comparisons to be made.

2.3 Samples

Each cross sectional slice through the tree trunks, W-1 to W-10, had regions of varying quality, some completely clear, some with different stages of fungial attack. From each of these larger slices, we cut small, smooth pieces, approximately 1 x 1 cm^2 in area from areas we considered to be representative of the various defects found on the slice.

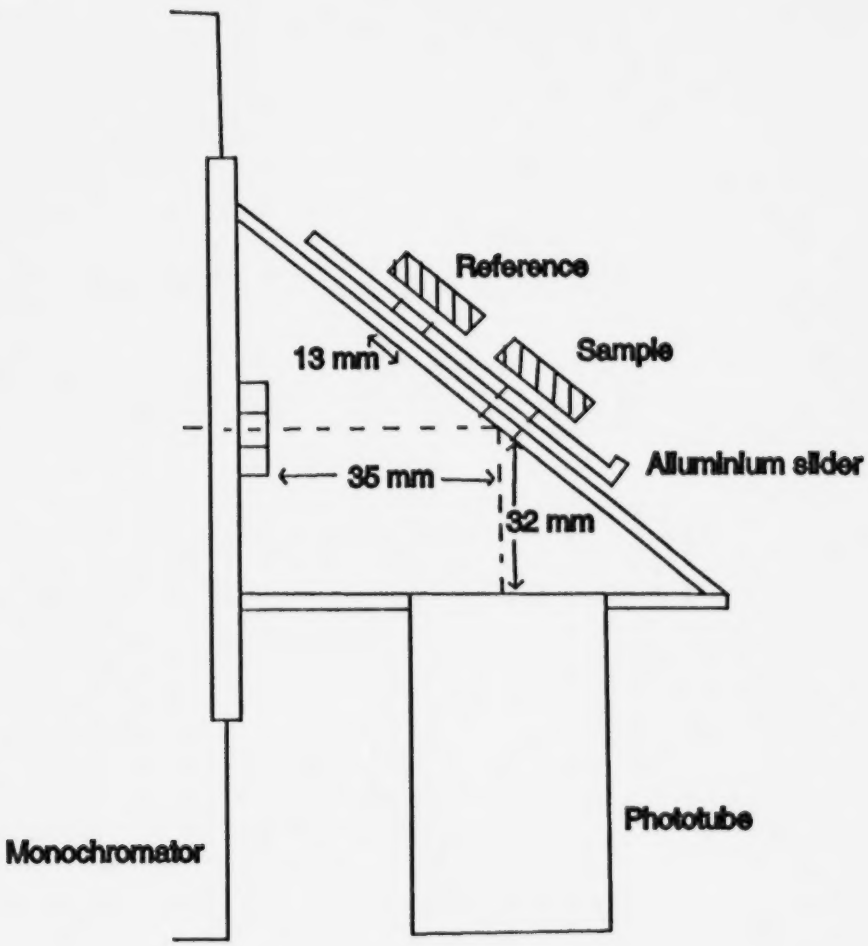

Figure 6

Schematic diagram of sample holder and assembly
for reflection measurements

2.4 Results and Discussion

The most uniform, whitest cross sectional slice, W-4, was selected as a standard. Its reflection was measured against a white ceramic surface (figure 7). Since we were interested in determining deviations from "clear" aspen wood in the defective material , we subsequently made all further reflection measurements with a sample of W-4 as the reference standard. Different samples from W-4 when compared to each other agreed in reflection properties to within one percent.

Reflection measurements on W-3, W-5 W-8, and W-9 vs wavelength are shown in figures 8, 9, 10, and 11. All curves, except W-3 which has black patches, show that the relative reflected intensity for the discolored wood is lower than for the clear wood. According to Hiratsuka (table 4), W-3 and W-9 wood samples are classified as type A and W-5 and W-8 wood samples are classified as type C. Although reflection intensities with respect to the clear aspen wood decrease with decreasing the wave length, there is again an increase in the violet and near UV region with a minimum around λ = 450 nm. The sample taken from W-3 which has black figuring (Type A) was different from light brown and rot in the same wood slice. Its reflection intensities increase with decreasing wavelength over the entire range as compared to the clear wood. The surface of that sample, W-3 with black patches, was very smooth and harder than the other two samples of W-3.

In addition to the samples described above, other samples were also examined for reflection characteristics. Intensity curves of brown in W-6 and brown in

W-10 were the same as the brown in W-8. A clear sample of W-10 with light brown patches had the same characteristics as W-3 with black patches. The greatest deviation of reflection intensities between brown wood and clear wood is in the blue region of the spectrum where the clear wood has higher reflection intensities than brown wood by as much as 50%.

Since it was important to know whether the reflection intensities with respect to the clear aspen wood depend on the smoothness of the wood sample, some samples were tested after sanding by different grades of sand paper. Although reflection intensities of freshly sawn W-7 - sample measured with respect to the clear wood decrease with the wavelength, reflection intensities of a sample after being sanded by 240 sand paper continuously increases with decreasing the wavelength similar to the sample of W-3 with black patches (See figure 8). When the surface of the wood is sanded, the reflection of light is the result of scattering due to small particles. Since the scattering depends on the inverse of fourth power of wavelength, the reflection intensity increases with decreasing the wavelength. When the sample is sanded, the spacings of the wood fibers on the surface of the samples are covered by the small wood particles. Due to that fact, the amount of light which enters the wood along the fibers decreases and reflection due to scattering increases. Therefore, reflection is higher when the sample is sanded and increases with decreasing of wavelength.

Also to check the effect of the grit size of the sand paper used for the sanding, one sample sanded with 240 grit carborundum and an other with the very coarse 50 grit garnet were compared with respect to reflection intensities. There were

no noticeable differences between them. In both cases, the spacings between fibers on the surfaces of the samples are covered by the particles of wood dust which decreases the light entering into the wood. Regardless the size of the wood particles made from 50 grit garnet and from 240 grit carborundum, all particles block the light which enter to the fiber. Also, the reflection due to scattering does not directly depend on the size of the particles. Therefore, the reflection intensities of the samples sanded by two different grades of sand paper are expected to be similar.

Moisture content is very important, because in light woods the weight of moisture may exceed by many times the weight of wood substance itself. Moisture is also subject to continuous variation when wood is exposed under varying atmospheric conditions. It was suspected that the reflection measurements of wood was depend on the moisture content of wood. Therefore reflection measurements, always with respect to the clear aspen wood, were taken for a light brown sample and then for the same sample after soaking it in water for one day. There was no noticeable difference in reflection measurements with respect to the clear standard W-4 sample before and after soaking in water.

In addition to measurements of reflection intensities of pieces of the sawn and polished wood slices, it was decided to use small chips of aspen wood from the pulp mill just before they enter the pulping process. Chips do not possess a specific shape or smooth surfaces. Here too we used W-4 as the standard. Two sets of reflection intensities of each were measured, one with incident light

hitting the surface along the grain; ie. the plane of the incident light and reflected light is parallel to the grain and the other with the light hitting across the grain; ie. the plane of incident light and reflected light is perpendicular to the grain. For a very clear chip reflection intensities are almost same for both the horizontal and the vertical grain measurements with respect to the incident light. For a stained chip, the reflection intensities of vertical grain measurements are higher than that of horizontal grain measurements with respect to the incident light.

The results of reflection measurements from chips were basically similar to the reflection measurements from sawn wood samples. Reflection measurements from clear chips with respect to the clear aspen wood were the same as that of the clear slices. Reflection intensities of discolored chips as compared to the clear aspen wood decrease with decreasing wavelength and there is again an increase in the violet and near UV region with a minimum around $\lambda = 450$ nm, the same result as was found in the slices. When the color of the chips gets darker and darker, the slope of the curve in reflection intensities between 450 - 1100 nm increases gradually.

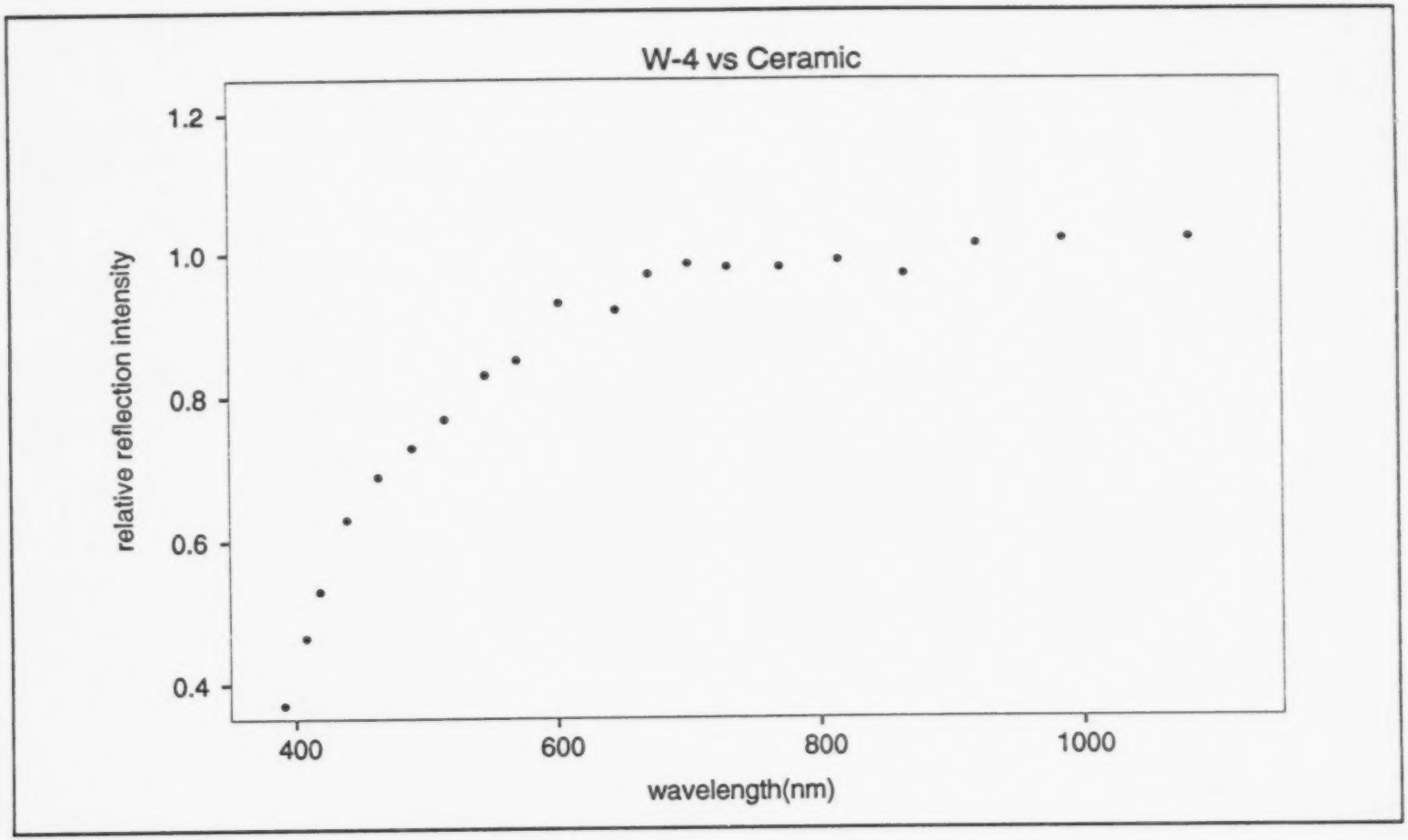

Figure 7 - Relative reflection vs wavelength for W-4 (vs ceramic)

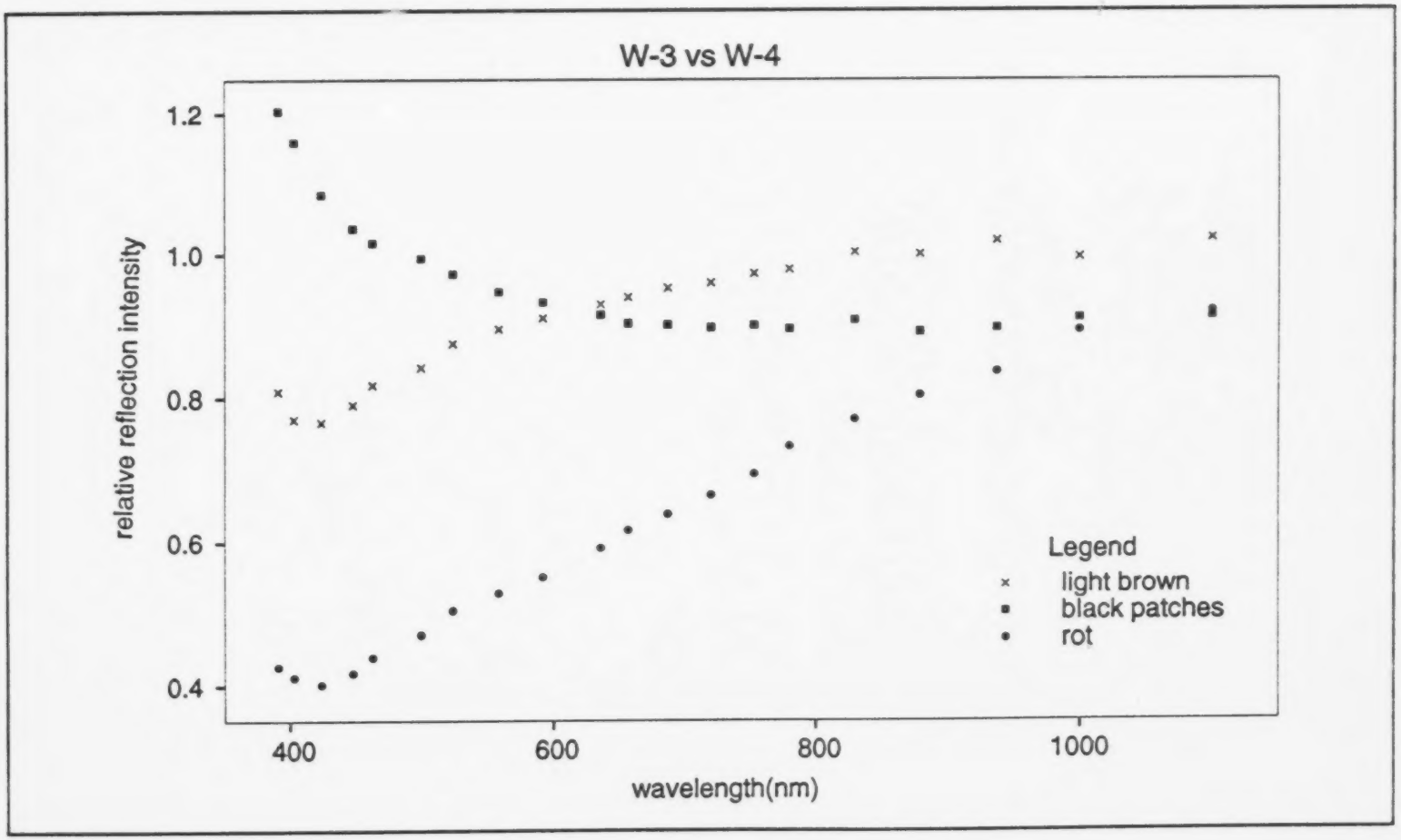

Figure 8 - Relative reflection vs wavelength for W-3

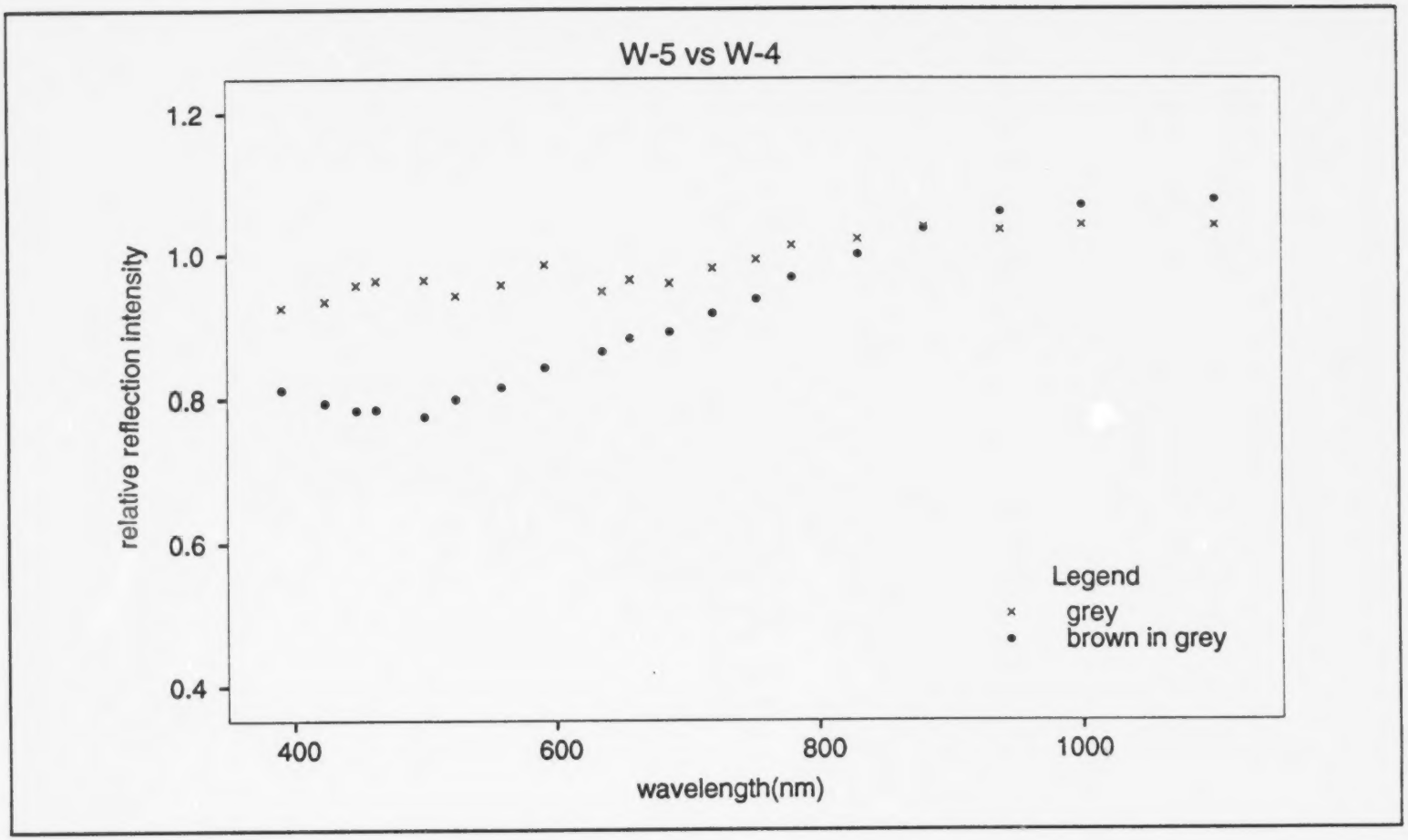

Figure 9 - Relative reflection vs wavelength for W-5

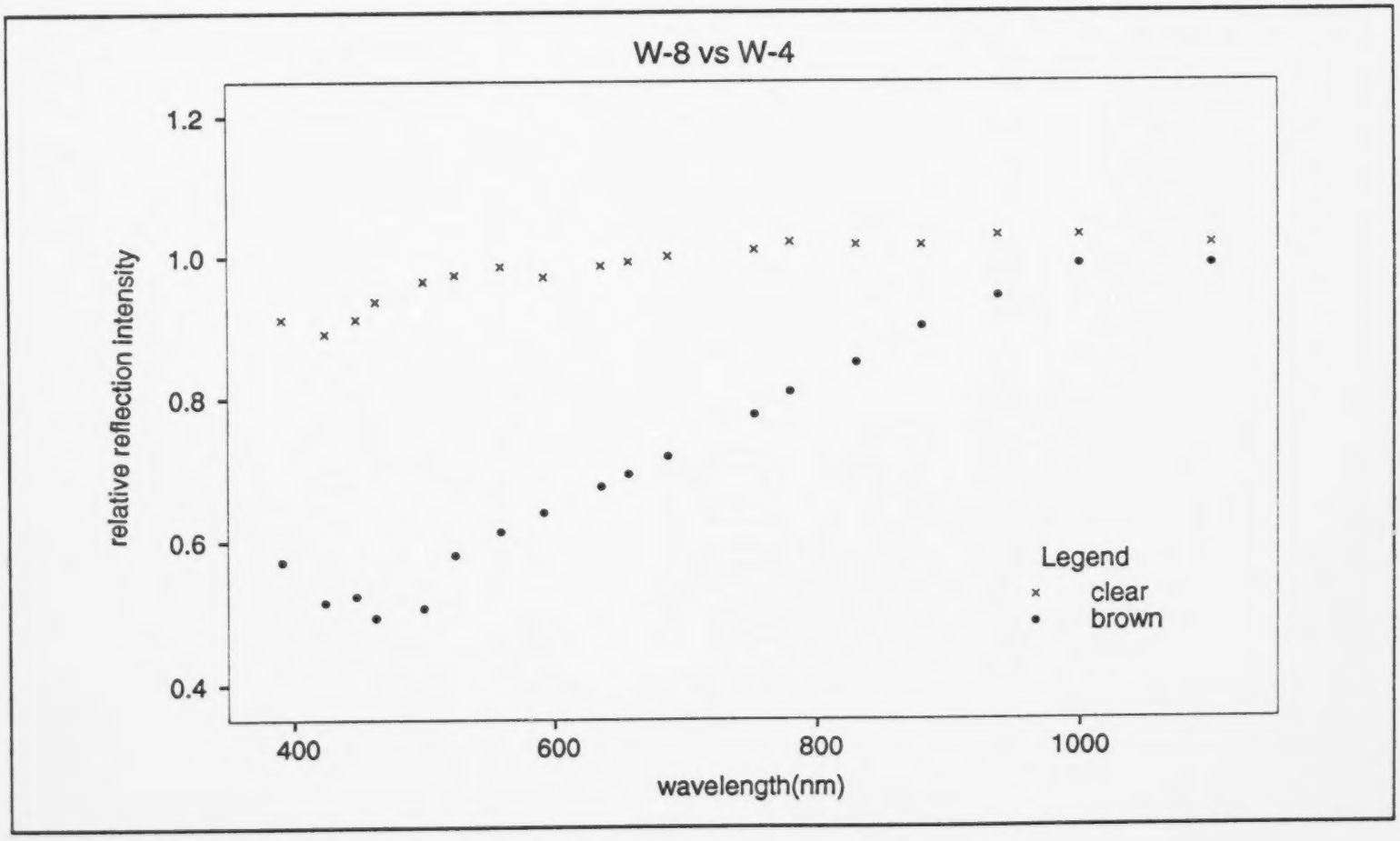

Figure 10 - Relative reflection vs wavelength for W-8

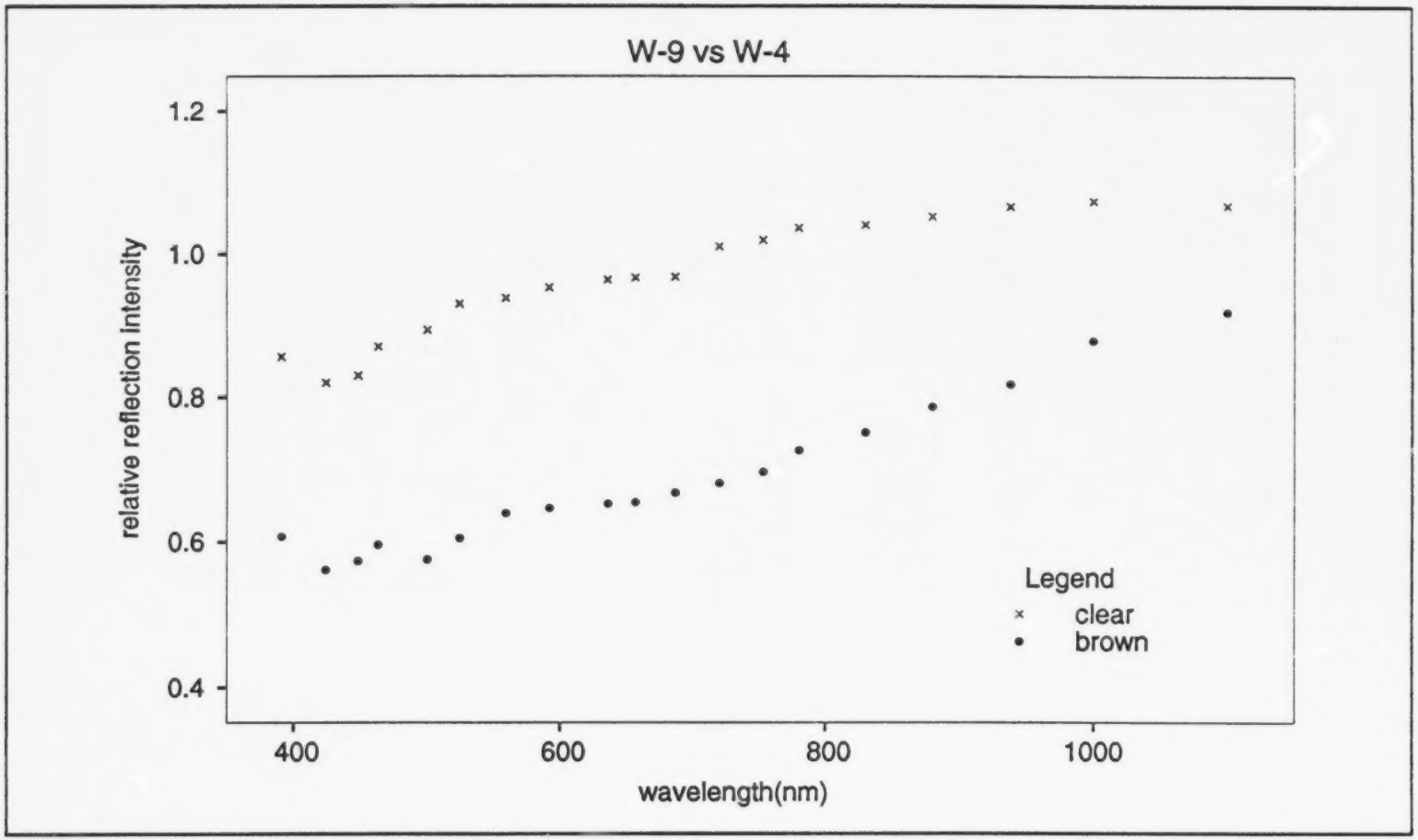

Figure 11 - Relative reflection vs wavelength for W-9

CHAPTER 3

Transmission Measurements

3.1 Background

While making luminescence measurements on various pieces of aspen wood (which will be described later) , it was noticed that He-Ne laser light penetrated as much as 1 cm of wood. The visibility of the laser light on the opposite side appeared to depend on both the direction of grain and the quality of the wood. Although transmission measurements are likely to be far more difficult to apply to automated monitoring of large quantities of wood than reflection measurements, it was considered to be of scientific interest to make a systematic investigation of transmission characteristics of sound and defective wood as a function of wavelength and direction of grain.

3.2 Equipment and Procedure

The experimental set-up for measuring transmission intensities is shown in figure 12. The equipment used for the reflection measurements was, except for the sample holder and the sample assembly, the same as that described in section 2.2 .

Sample Holder and Assembly

The sample holder was a slider of brass with a hole of 3 mm in diameter. The sample was glued on and behind the hole. The slider can be shifted by pulling or pushing on a wire. This assembly allowed the beam to pass either through a

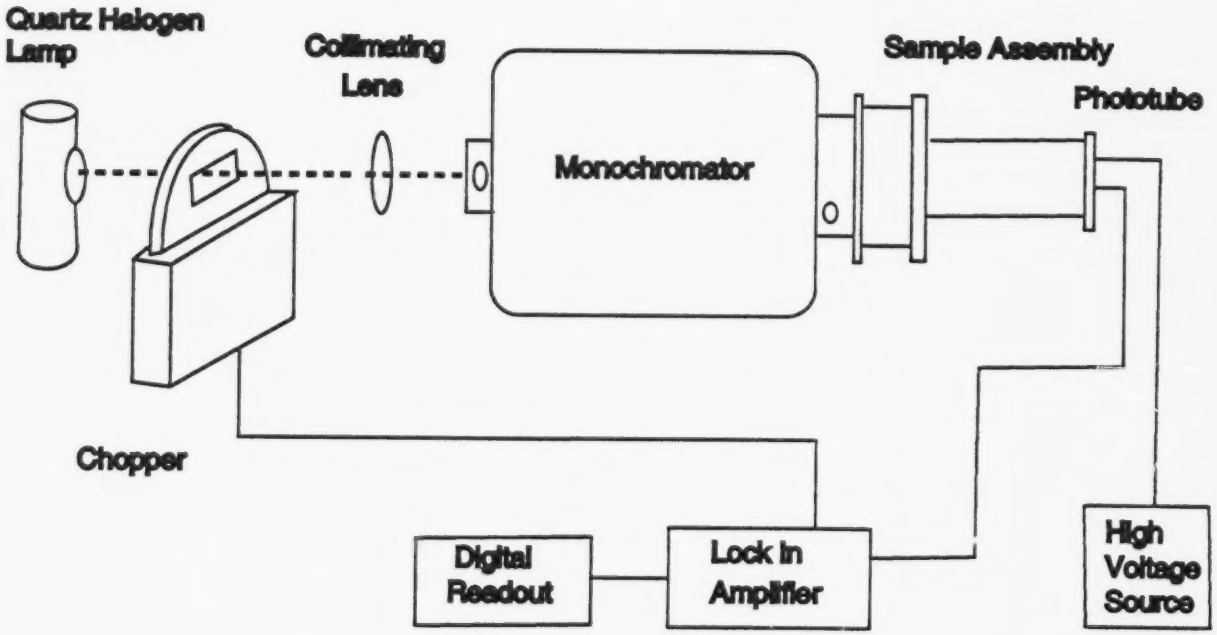

Figure 12 - Experimental setup for transmission measurements

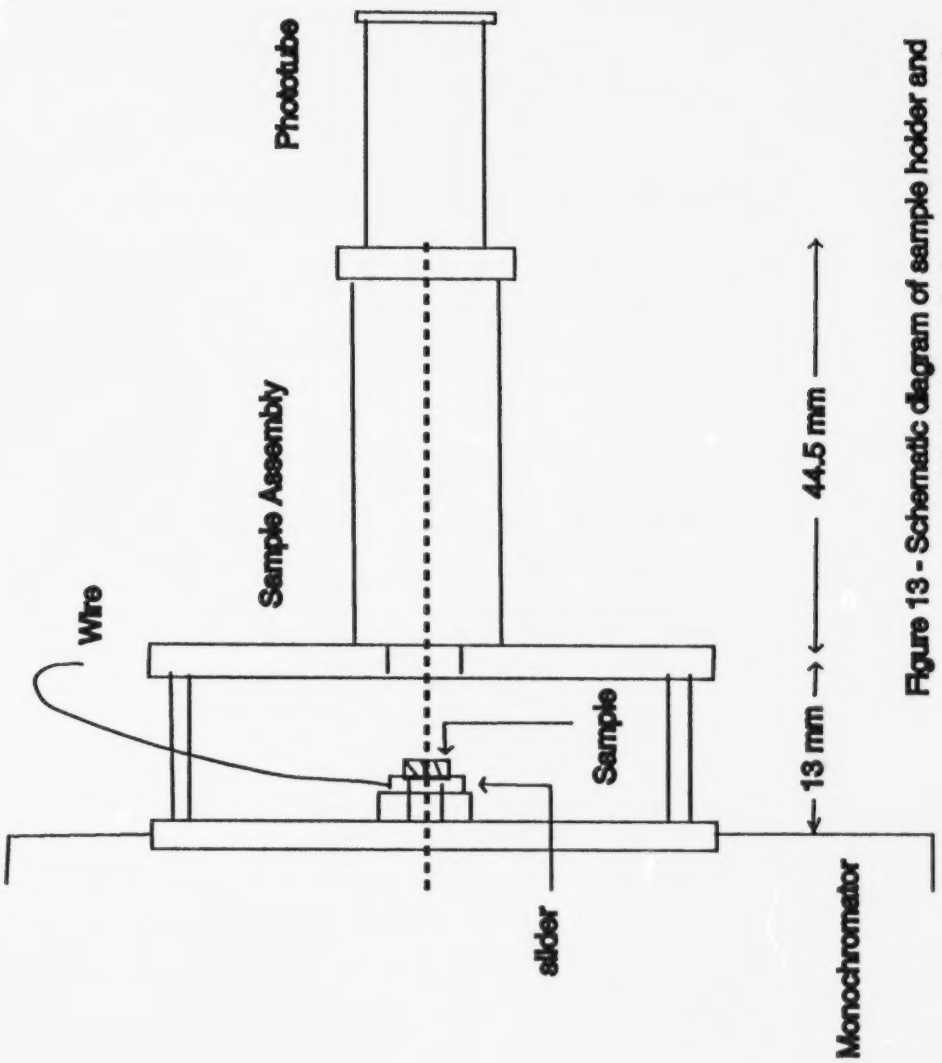

Figure 13 - Schematic diagram of sample holder and assembly for transmission measurements

wood sample or unimpeded through a 3 mm opening (figure 13). This allows the two factors of the transmission ratio to be measured within a short period.

3.3 Sample Preparation

For the transmission measurements we concentrated on segments of slice W-9. Since samples of more than 10 mm thickness do not give reliable transmission intensities to measure, we started with samples not more than 8.75 mm thick, and, after each set of measurements, reduced the thickness with sandpaper. Wood dust on the surface was removed by a blower.

We always took two samples from the same portion of the wood and cut them such that in one sample light travels along the grain, and in the other across the grain.

3.4 Results and Discussion

The behavior of transmission ratios with respect to thickness at different wavelengths for samples of the wood slice designated as W-9 is shown in figures 14, 15, 16, and 17. Figures 14 and 15 were obtained for the pieces of clear wood and figures 16 and 17 were for the discolored wood. Figures 14 and 16 show the results with the incident light along the grain, while 15 and 17 were measured across the grain.

It can be seen that there are striking differences in transmission for both clear and stained wood when the light enters along the grain as compared to entering across the grain. Light travelling along the grain is attenuated much less than light travelling across the grain which confirms the results of Mathews (1976).

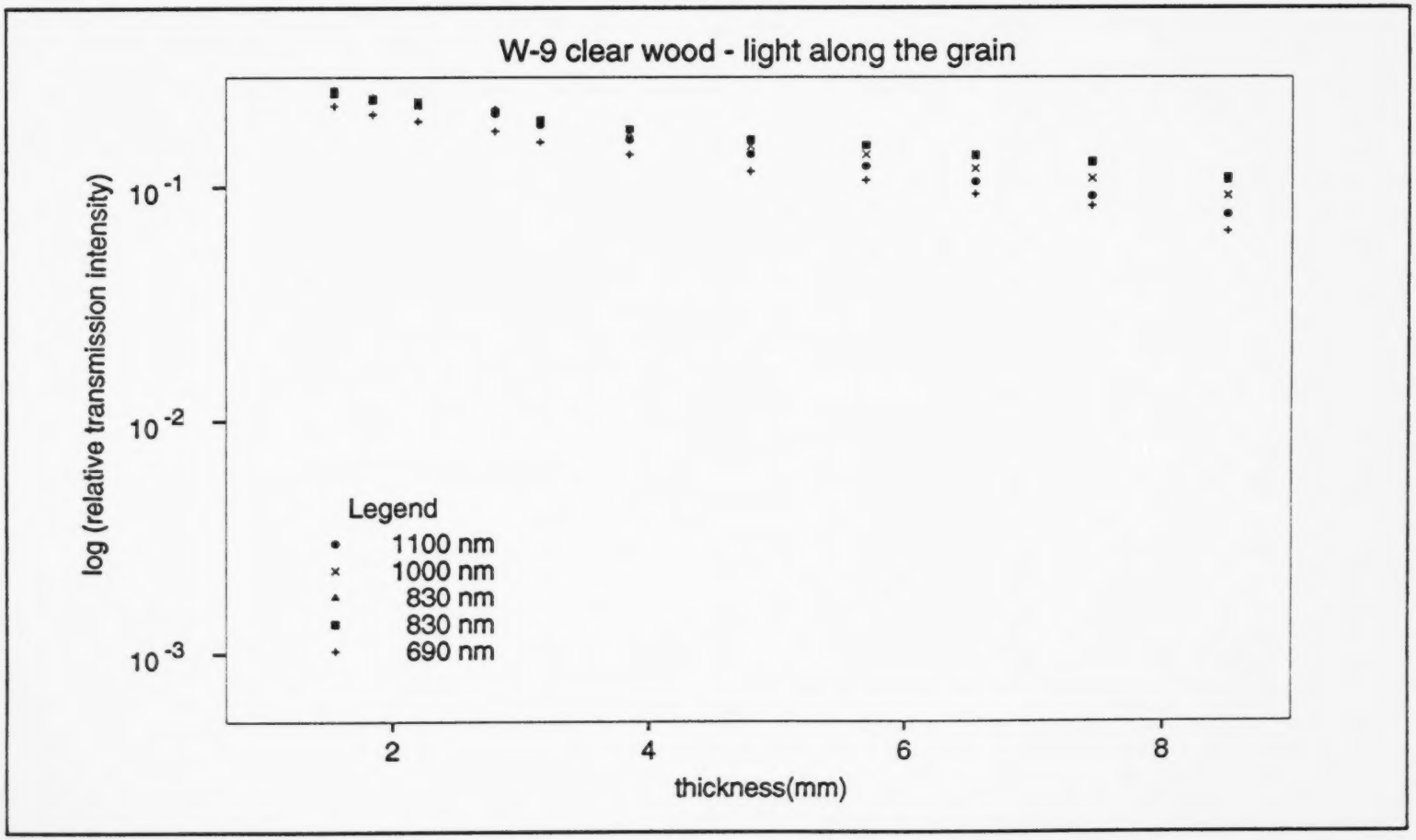

Figure 14 - Relative transmission vs wavelength of w-9 (clear wood, light along the grain)

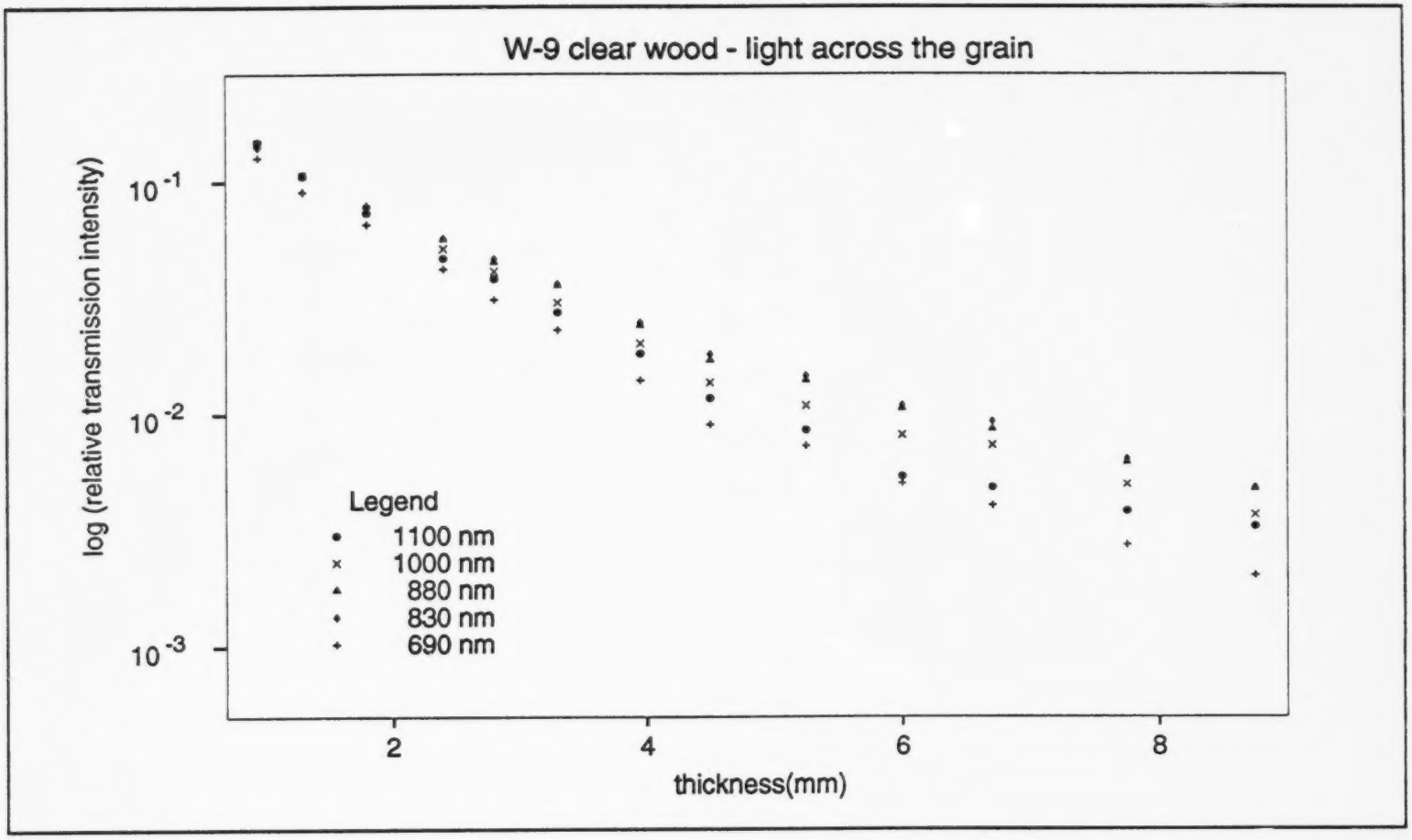

Figure 15 - Relative transmission vs wavelength of w-9 (clear wood, light across the grain)

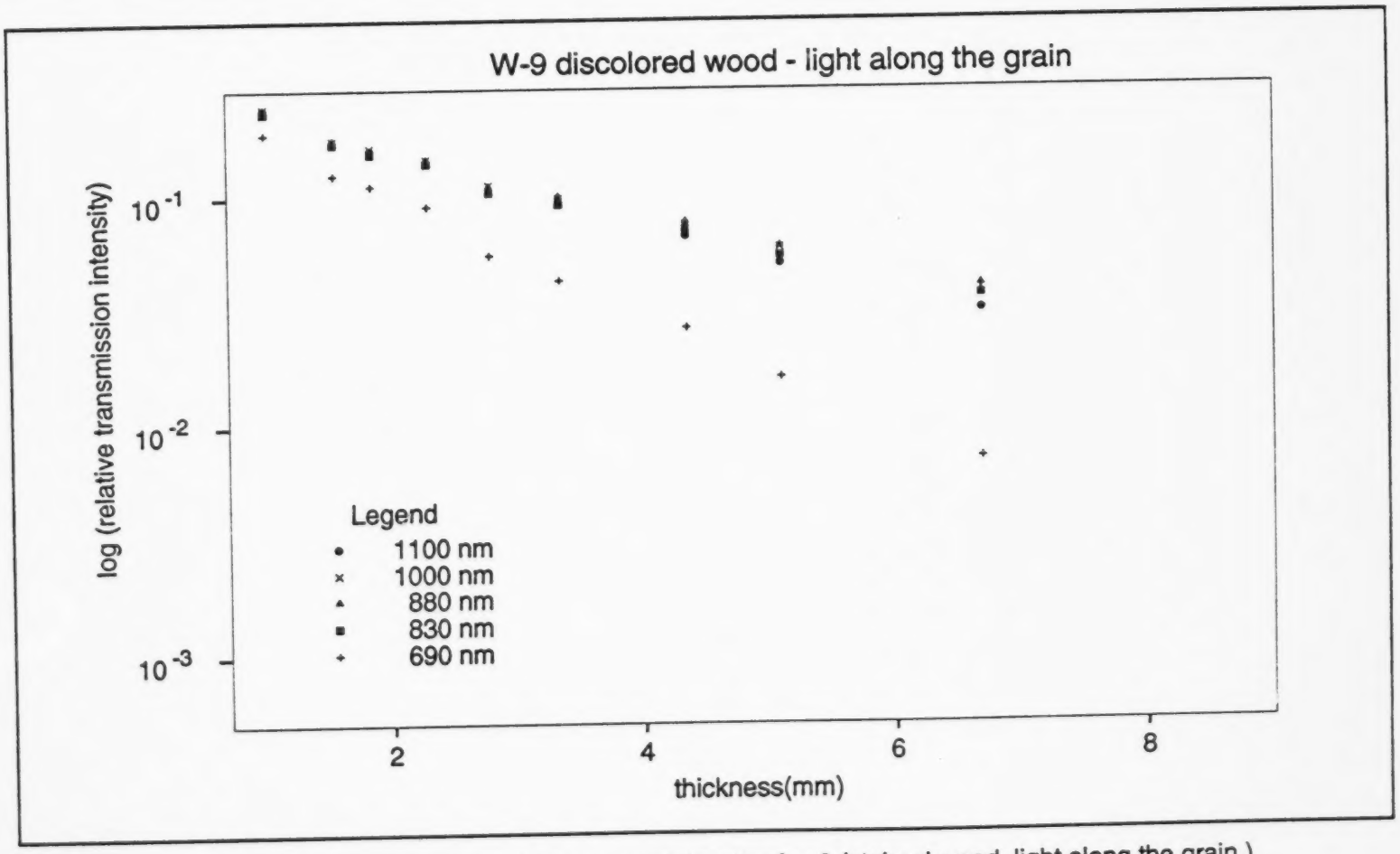

Figure 16 - Relative transmission vs wavelength of w-9 (stained wood, light along the grain)

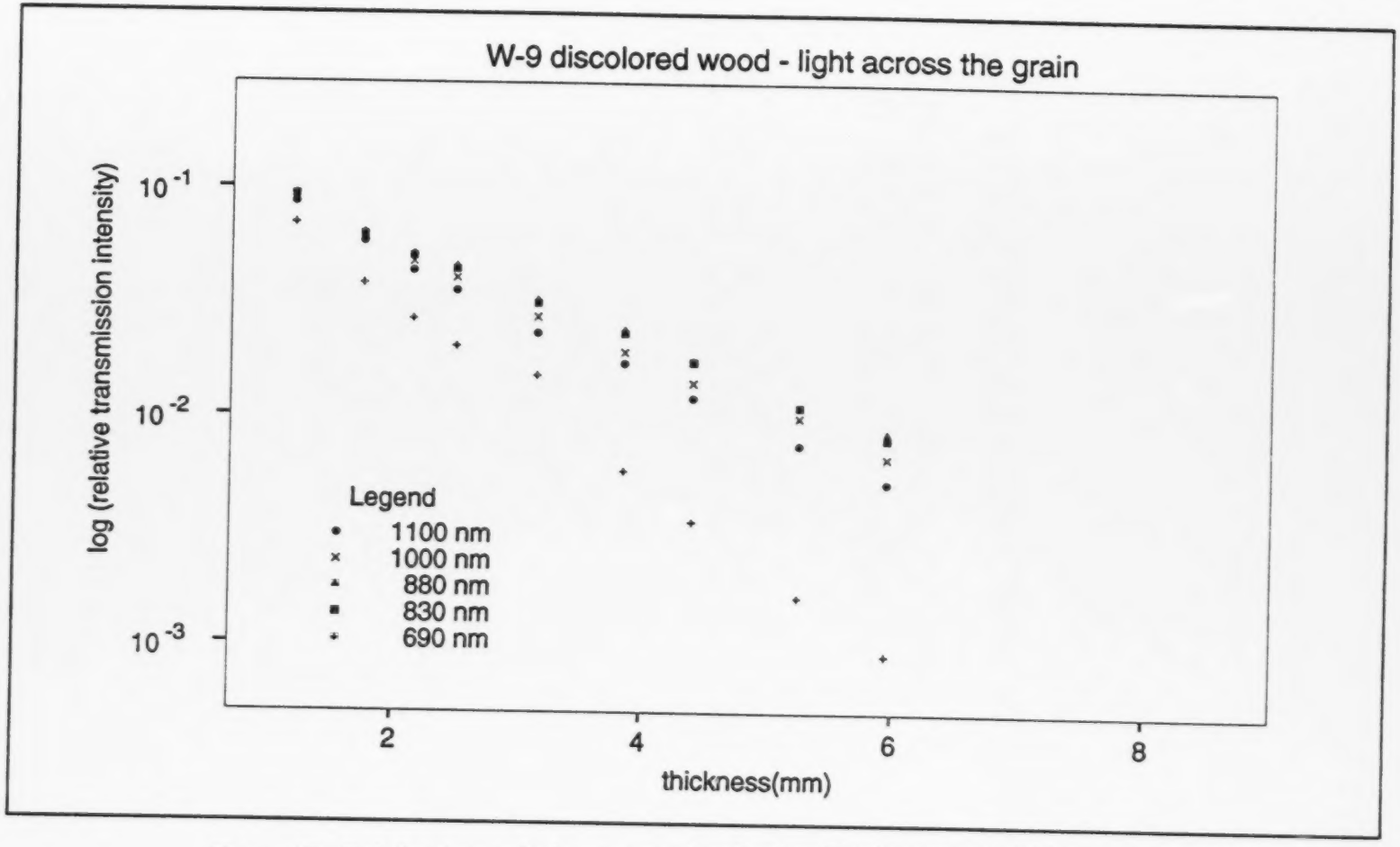

Figure 17 - Relative transmission vs wavelength of w-9(stained wood, light across the grain)

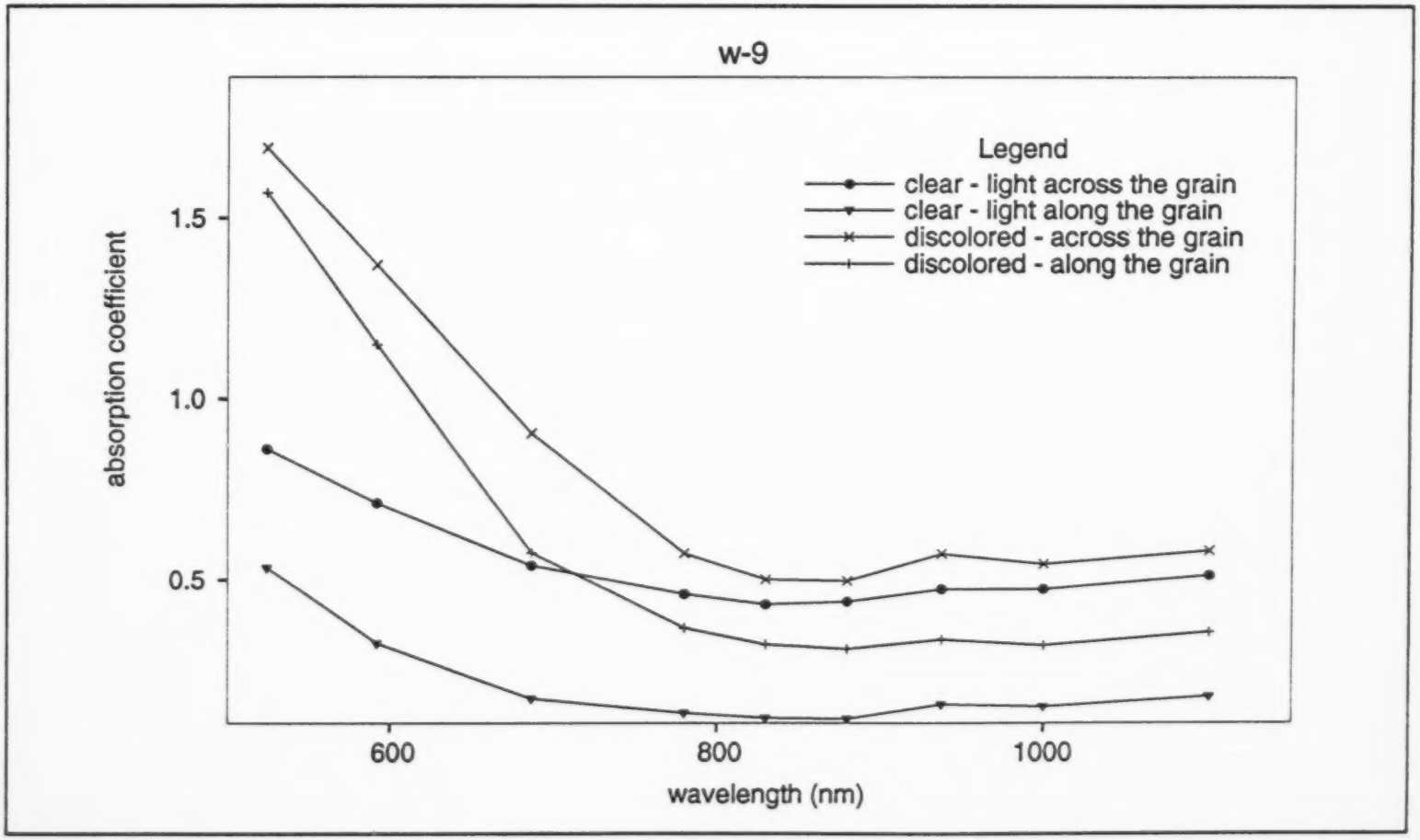

Figure 18 - Absorption coefficient vs wavelength for w-9

For the discolored wood samples, transmission ratios are very difficult to measure for thicknesses greater than 6.7 mm. The variation of absorption coefficients of W-9 vs wavelength is shown in figure 18. Absorption coefficients (α) were calculated according to the following equation.

$$I = I_o e^{-\alpha t}$$

I = transmitted intensity

I_o = incident intensity

t = thickness of the sample in mm

α = absorption coefficient in mm^{-1}

For clear wood the two curves for incident light along the grain and across the grain, behave in the same manner as a function of wavelength, but there is a consistently higher absorption coefficient for incident light across the grain. It can also be noticed that for the wavelength shorter than 690 nm, the discolored wood has a higher absorption coefficient than clear wood. All four curves showed higher absorption coefficients for shorter wavelengths.

3.5 Transmission Analysis

We have constructed a model to do a computer simulation of the transmission of light through wood.

3.51 Assumptions

Due to the complicated structure of the wood, we made the following simplifying assumptions,

i. Wood consists of a single cell type, henceforth referred to as fibers (even though all wood mass is made up of a variety of different cells called fibers, vessel members, and parenchyma cells) and even though light transmission may occur more through the other types of cells (vessel members) than fibers.

ii. Wood fibers are cylindrical in shape and they are aligned parallel to the tree as shown in the figure 19.

iii. The diameter of the wood fiber is greater than the wavelength of the incident light.

iv. Wood fibers consist of an isotropic, transparent, and homogeneous medium.

3.52 Calculations

As shown in figure 20 , it was assumed that light rays enter each fiber as a parallel beam perpendicular to the axis of the cylinder. Furthermore, according to the basic laws of reflection and refraction, the incident, reflected, and refracted rays all lie in the plane of incidence. Therefore, for the calculations, only one plane, the plane of incidence, was considered.

When a plane monochromatic light wave is incident on a surface separating two isotropic media, its E (electric field) and B (magnetic field) can be resolved into components of parallel and perpendicular to the plane of incidence. In our calculations, only the case of E perpendicular to the plane of incidence was considered for simplicity.

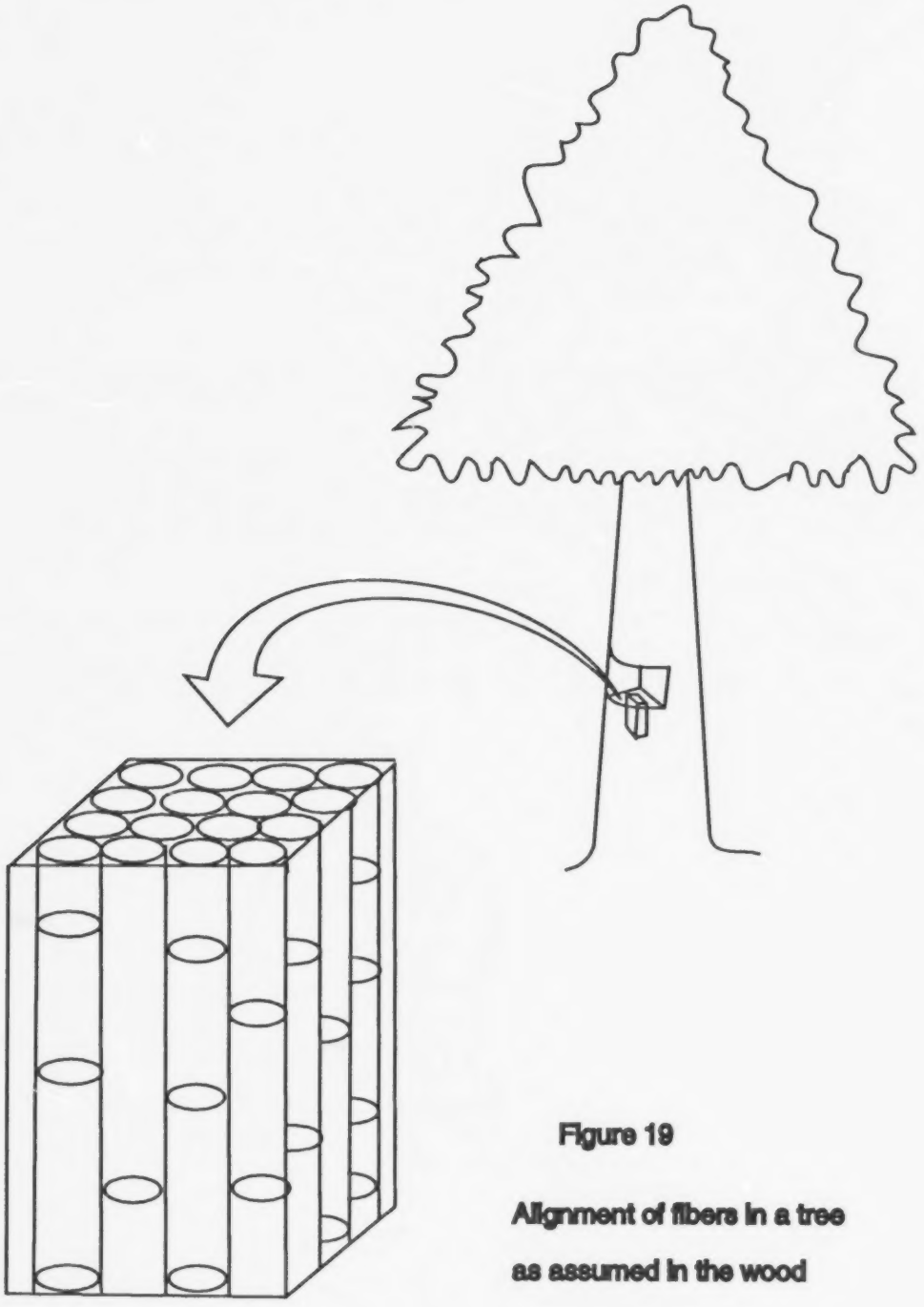

Figure 19

Alignment of fibers in a tree as assumed in the wood

For a light ray impinging on a surface with its E perpendicular to the plane of incidence, the amplitude of the reflection coefficient (r) and the amplitude of the transmission coefficient (t) are given by following expressions which are derived from Maxwell's equations.

$$r = \frac{n_i \cos\theta_i - n_t \cos\theta_t}{n_i \cos\theta_i + n_t \cos\theta_t}$$

$$t = \frac{2n_i \cos\theta_i}{n_i \cos\theta_i + n_t \cos\theta_t}$$

n_i = index of refraction of the incident medium

n_t = index of refraction of the refracted medium

θ_i = incident angle

θ_t = refracted angle

As shown in figure 20 , when the incident light enters the "fiber", part of it reflects while the other part refracts and penetrates the "fiber" where it undergoes numerous additional reflections and refractions. Since the "fiber" is assumed to be cylindrical in shape, the amount of incident light per unit surface area of the fiber is not the same along its circumference as shown in the figure 21. Hence the actual energy per unit area which strikes the surface is the beam intensity multiplied by the cosine value of the angle as measured with respect to the

direction of the incident light (Figure 21). The computer program written for intensity output calculations is given in appendix 1.

3.53 Results and Discussion

Since the intensity of the light is greatly reduced by the reflections and refractions due to the reflection coefficient (r) and the transmission coefficient (t), only the first few terms were considered for calculations.

Refractive index n_i was taken as 1 (for air) .

The graph for relative transmitted intensity from the fiber against the angles (0° - 360°) measured with respect to the direction of incident light is shown in figure 22. Since the refractive index of wood is unknown, the calculations were made for refractive indices (n_t's) 1.3, 1.5, and 1.7. It can be seen that the transmission is highest at the angles where the light travels straight through the fiber.

The relative light intensity after the first external reflection and the transmitted light intensity after the first, second and third internal reflections can be seen in figure 23 where the calculations were made for n = 1.5. The highest relative transmitted intensity including the peak forward intensity is given by the transmission after the first internal reflection. The relative transmitted intensity after the third internal reflection is considerably smaller. The total relative transmitted intensity which was calculated by adding the intensity in each 6° intervals can be seen in the figure 24. The discontinuities of the transmitted intensities in figure 24 can be explained; ie. the transmission at the first internal reflection does not occur at some angles at which the first external reflection occur.

If we take the transmitted light which comes out within 15° of the incident light direction, we get an approximate value of 40% of the intensity. Now assume that the light rays which come through within 15° of the incident light direction are close to being parallel to the incident light. If that 40% of transmitted light from the first fiber at the first layer hits the second fiber at the second layer, again 40% of second fiber's incident light will be transmitted to the third fiber at the third layer.

If we take $\alpha = 0.75\ mm^{-1}$ (from the figure 18), the thickness of a single fiber can be calculated using the following equation which was introduced in section 3.4 ;

$$I = I_o\, e^{-\alpha t}$$

$$\alpha t = -\ln (I / I_o)$$

where $I / I_o = 0.4$ for $n = 1.5$ and t = thickness of a single fiber layer

Calculated value for the thickness of a single fiber layer = 1.2 mm

The light which travels at angles greater than 15° of the incident light direction is considered to be scattered in the wood.

For completeness of the calculations, an absorption coefficient of the wood should also be included since real wood is not perfectly transparent even though we assumed it to be so in our calculations for the sake of simplicity.

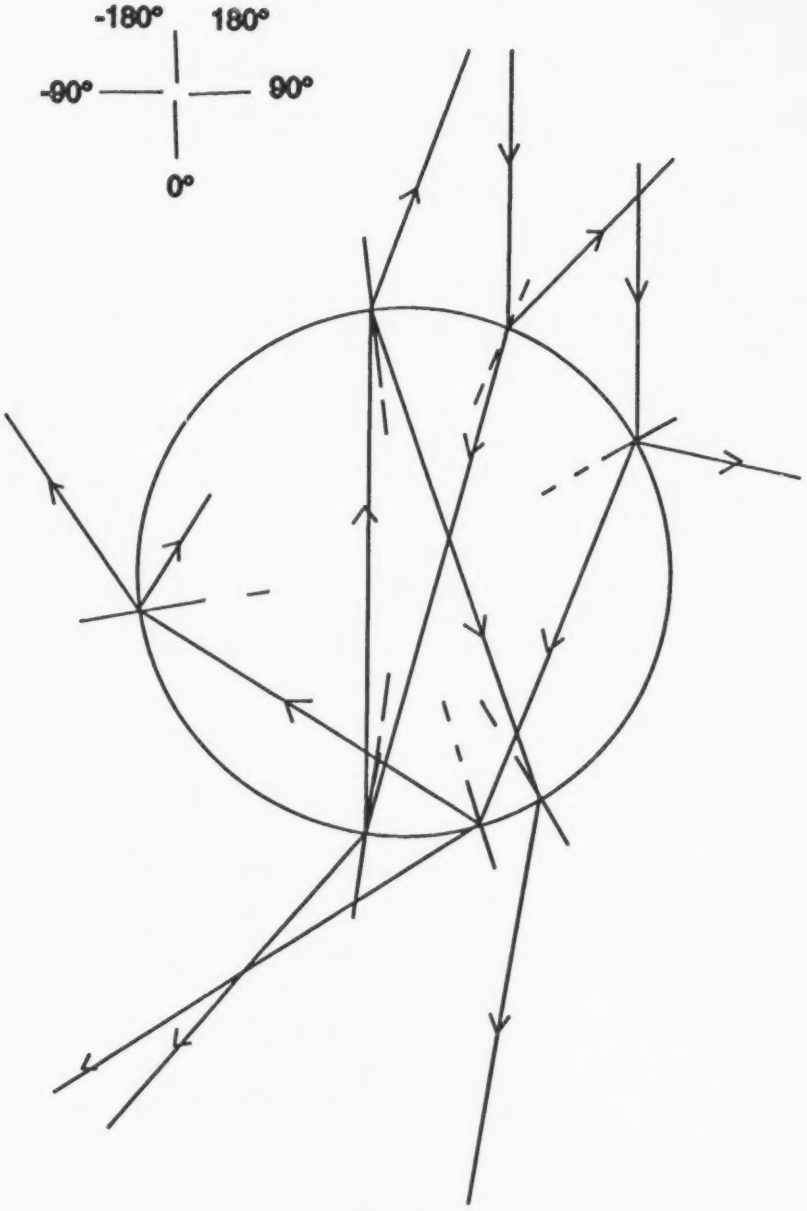

Figure 20

Light paths in an isotropic, transparent cylindrical rod

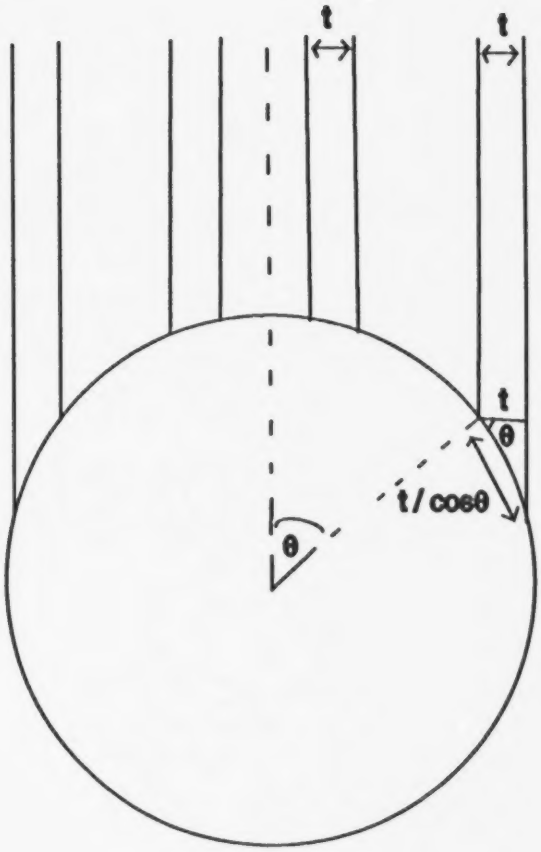

Figure 21

Decrease of energy for two arbitrary incident light rays per unit area with respect to the angle of incidence

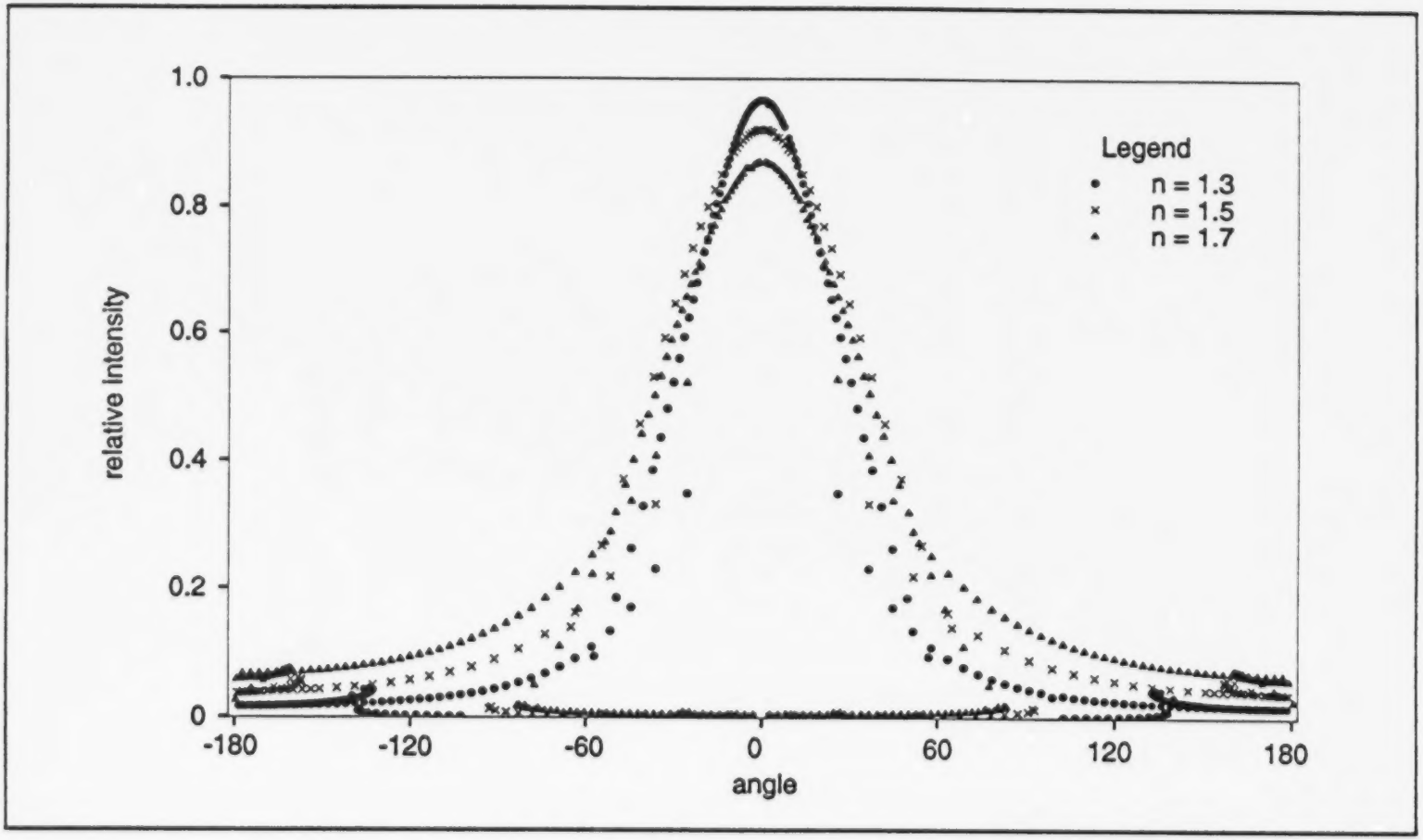

Figure 22 - Relative transmission vs angle measured with respect to the incident light

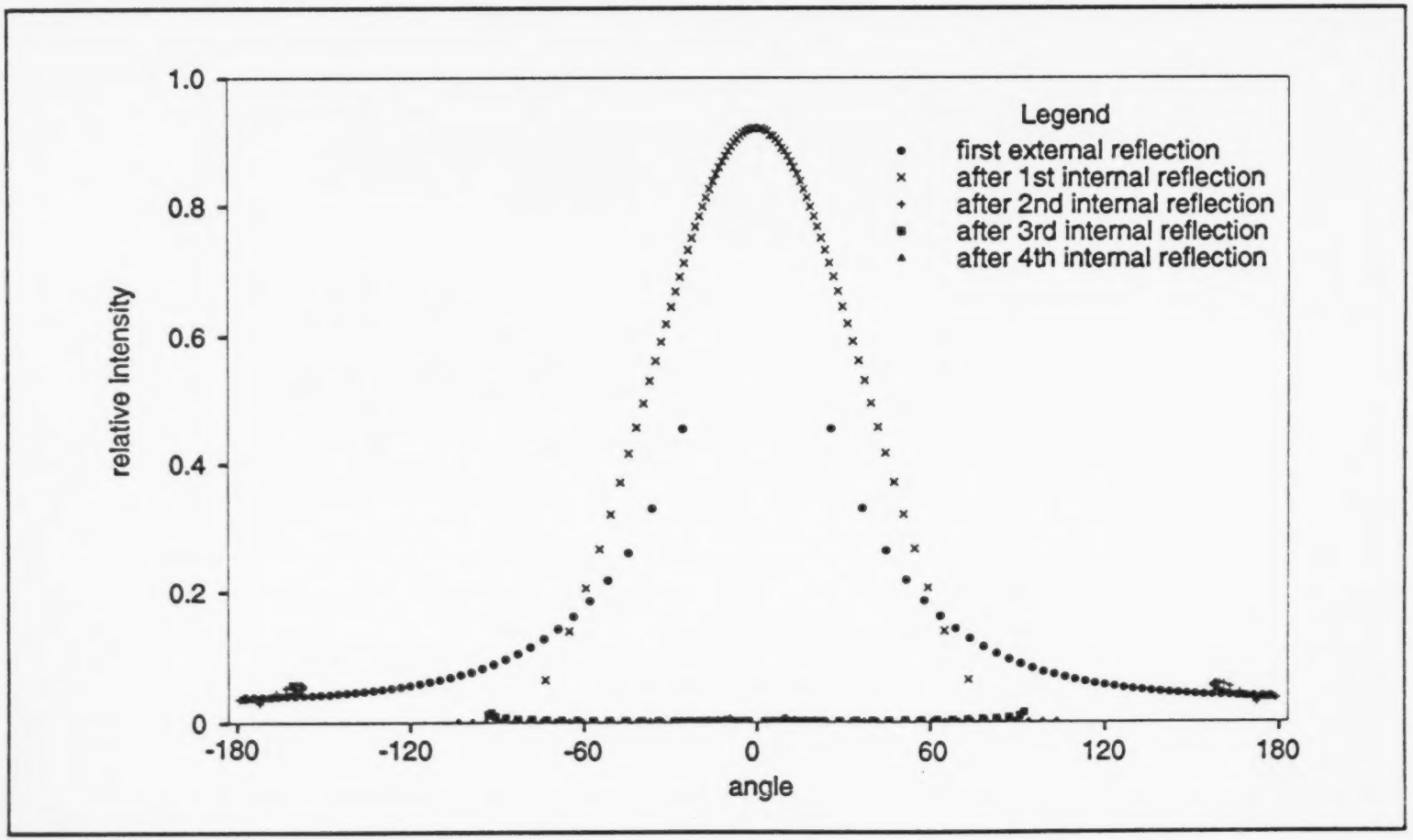

Figure 23 - Relative transmission vs angle measured with respect to the incident light

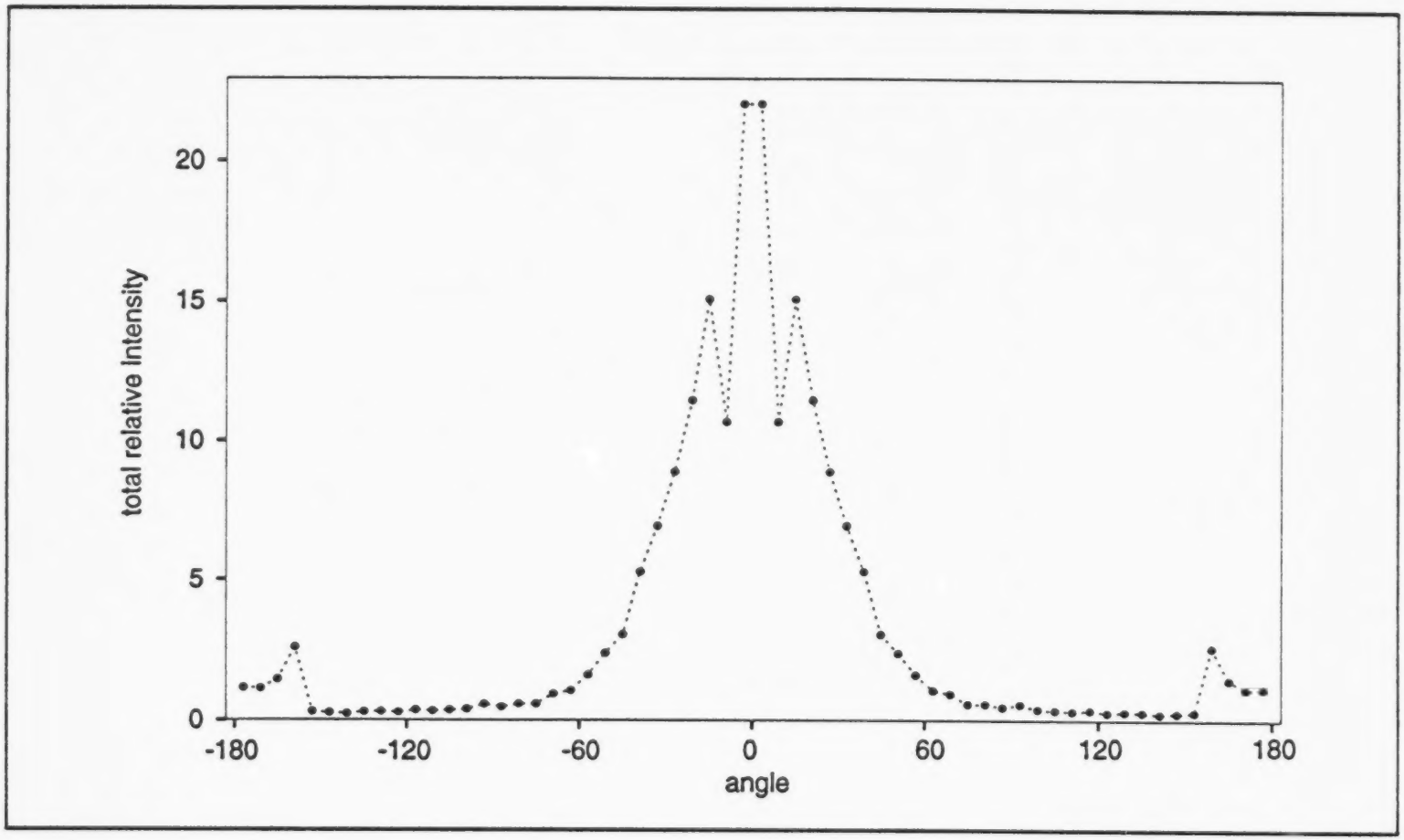

Figure 24 - Relative total transmission vs angle measured with respect to the incident light

CHAPTER 4

Luminescence Spectroscopy

4.1 Background

It is well known that some wood will luminesce under UV excitation after fungal attack. (Herring, 1978) This luminescence is in fact easily seen as a yellowish glow in the dark when the wood is exposed to a UV source.

The question we wanted to answer is if different defects in aspen have a different response in either the wavelength or the response time which could be used to distinguish between defects and adapted for automated defect recognition.

4.2 Equipment and Procedure

The luminescence intensity and the decay time were obtained by using the experimental setup illustrated in figure 25.

Monochromator

The MP1018B (Pacific Instruments) monochromator uses the reflective diffraction properties of a grating to spread out the spectrum of the incident light. This is in accordance to the grating equation ;

$$d (\sin \theta + \sin i) = n\lambda$$

d - the distance between lines

θ - the angle of diffraction

i - the angle of incidence

λ - the wavelength of the beam of interest

n - the order of diffraction

Detectors

i Photomultiplier

The detector was an S-1 response PMT (RCA 7102) working at 1200 volts delivered by a high voltage power supply (Northeast Scientific Company, model RE-2002). During the experiment, dry ice was used to cool the PMT to reduce the noise. The response curve for a typical S-1 tube can be seen in figure 5.

ii. Photodiode

A photodiode was used as a trigger to measure the arrival time of the laser pulse.

Laser

The excitation source used was a nitrogen laser (model PRA LN 1000) with pulse duration of 1ns and maximum repetion rate of 10 pulses per second. Wavelength of the laser was 337 nm.

Data acquisition system

The data acquisition system basically consisted of a peak detector, an 8-bit analogue-to-digital convertor (ADC), a monochromator drive unit, and a computer.

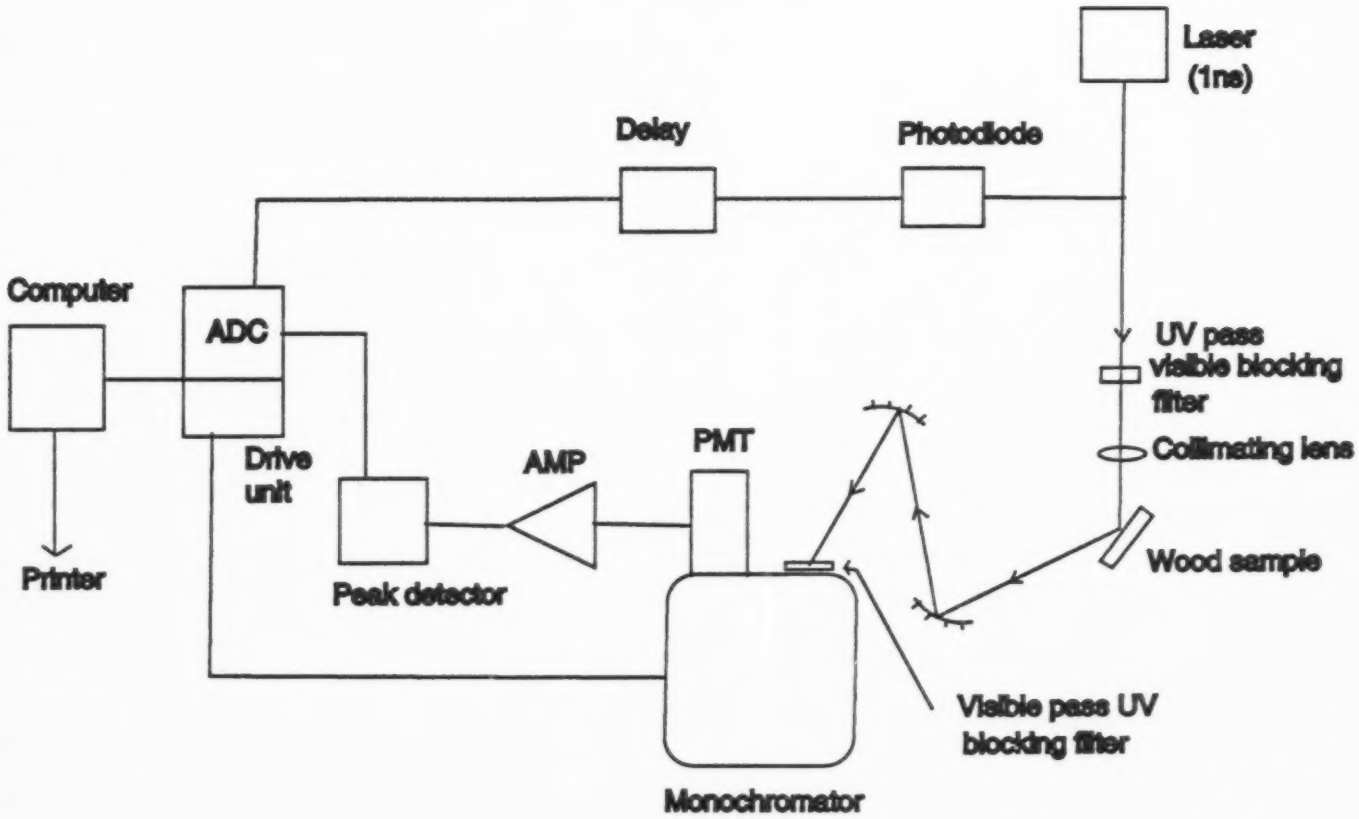

Figure 25 - Experimental setup for luminescence measurements

The data acquisition sequence involved the amplification of the output current from the photomultiplier, followed by finding and holding the maximum level for a sufficient length of time to allow for analogue-to-digital conversion by an ADC. Typical 8-bit conversion time was less than 20 μs. At the end of the conversion, the datum was stored by the computer. Data could be accumulated for a preset number of laser triggers for a particular wavelength setting, on completion of which, the data were sent to the computer (TKD 8006952, Wugo Technology) for storage. At the end of data transmission, the whole sequence was repeated at a new wavelength setting selected by the computer, until the final wavelength (preset by the operator) was reached. This system enabled the whole emission spectrum to be collected automatically.

4.3 Samples

Since all spots on the edges of the discolored parts of the slices did not give the same luminescent intensity, we chose as our samples those which gave the highest luminescence under UV excitation. Therefore, from among discolored wood samples described in Table 3, we used pieces of discolored wood from the slices designated as W-3, W-7, W-8, and W-9 for our luminescent measurements.

4.4 Results and discussion

4.41 Luminescence Intensity

After amplifying the output signal of the PMT and converting it to a binary signal by the ADC, the luminescent intensity was recorded with the wavelengths in the

computer. The wavelength range investigated was from 500 to 620 nm. A UV pass, visible blocking filter (corning glass CS 7-37) was placed in the incident beam to eliminate visible light falling on to the sample. 5 mm thick plexi glass was placed in front of the monochromator in order to block UV while allowing visible light to pass through. Since the readings of the luminescence intensities depend upon the wavelength sensitivity of the phototube, the measured intensities were corrected by using the sensitivity curve of the PMT (figure 5). Luminescence intensity curves representing W-3, W-7, W-8, and W-9 are shown in figure 26. The maxima of the W-3, W-8, and W-9 curves were normalized with respect to W-7. It can be seen that all the curves have maximum intensity around 535 nm. Even though the fungi are said to be different in different stained samples, the samples exhibit the same shapes in emission spectra and the maximum luminescence intensity occurs at the same wavelength. Therefore, the luminescence byproducts in decayed wood are very likely the same regardless of the fungi involved.

4.42 Decay Time

At the wavelength of maximum intensity, we attempted to measure the decay time at room temperature and liquid nitrogen temperature using a high speed digital oscilloscope (Tektronix TDS 420). The graphs obtained for the decay at 535 nm are shown in figures 27, 28 at room temperature and in figures 29, 30 at liquid nitrogen temperature for W-3 and W-7. In both graphs, the decay times were too short (1 to 2 ns or less) to be resolved satisfactorily. It was noticed that there was higher luminescence intensity when we cooled the samples to the liquid nitrogen temperature, but there was no noticeable change in decay time.

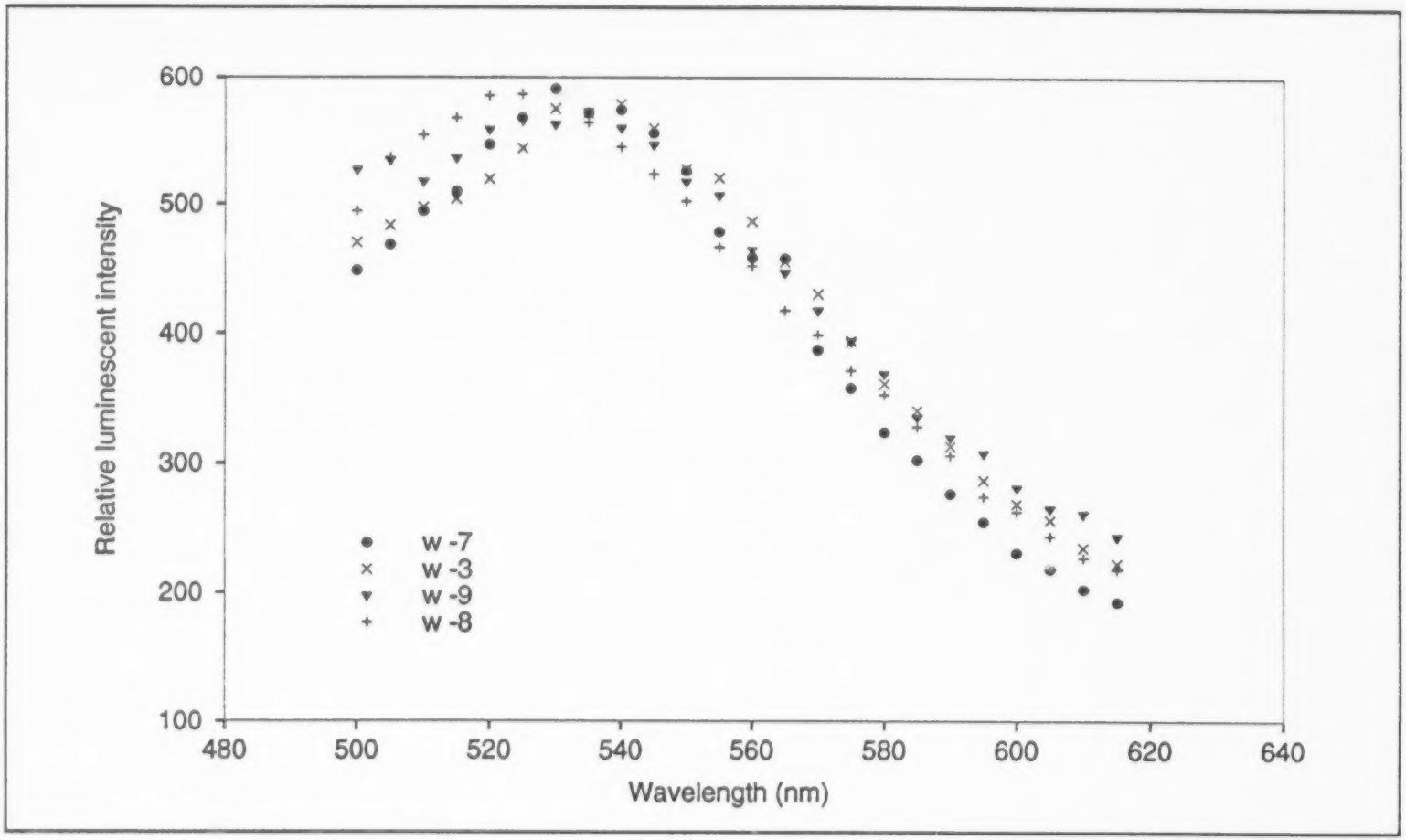

Figure 26 - Relative luminescence intensity vs wavelength

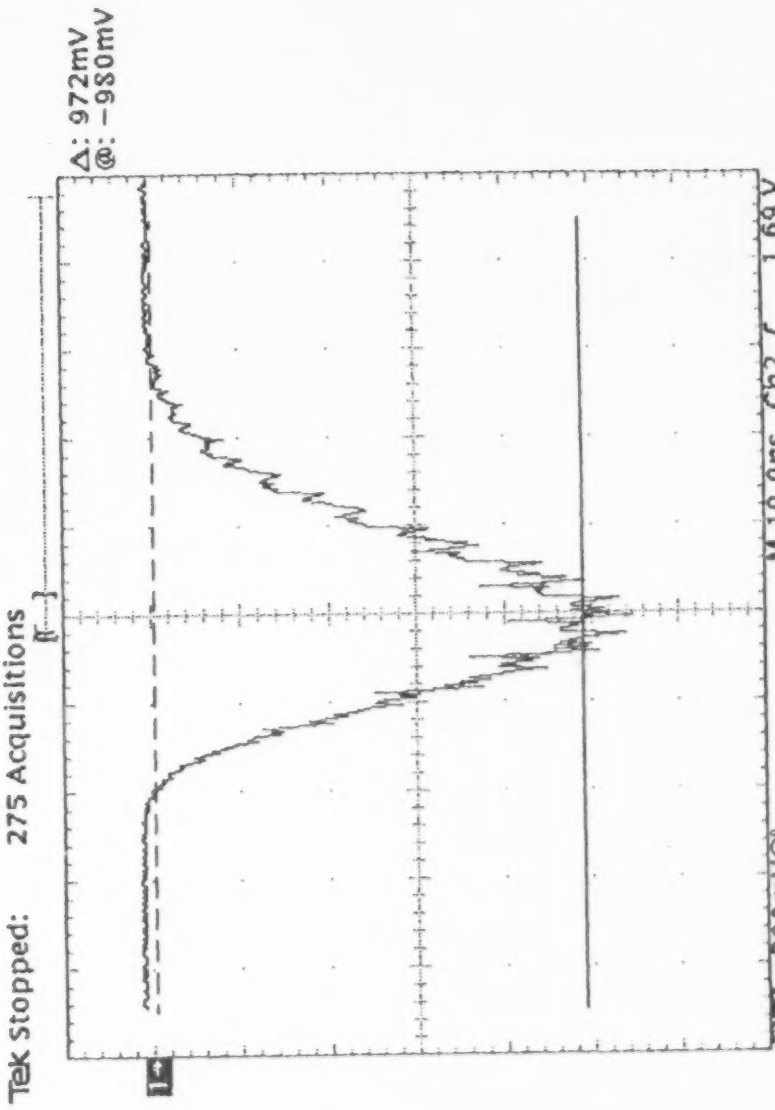

Figure 27 - Decay curve (w-3, room temperature)

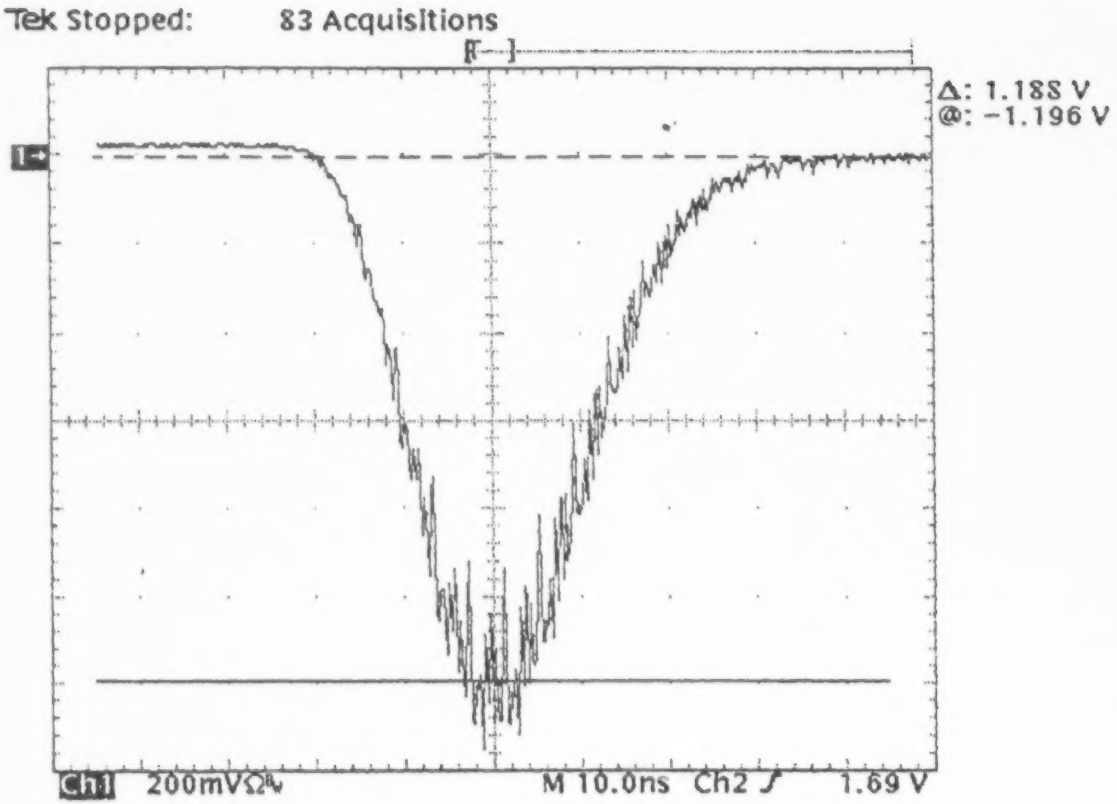

Figure 28 - Decay curve (w-3, liquid nitrogen temperature)

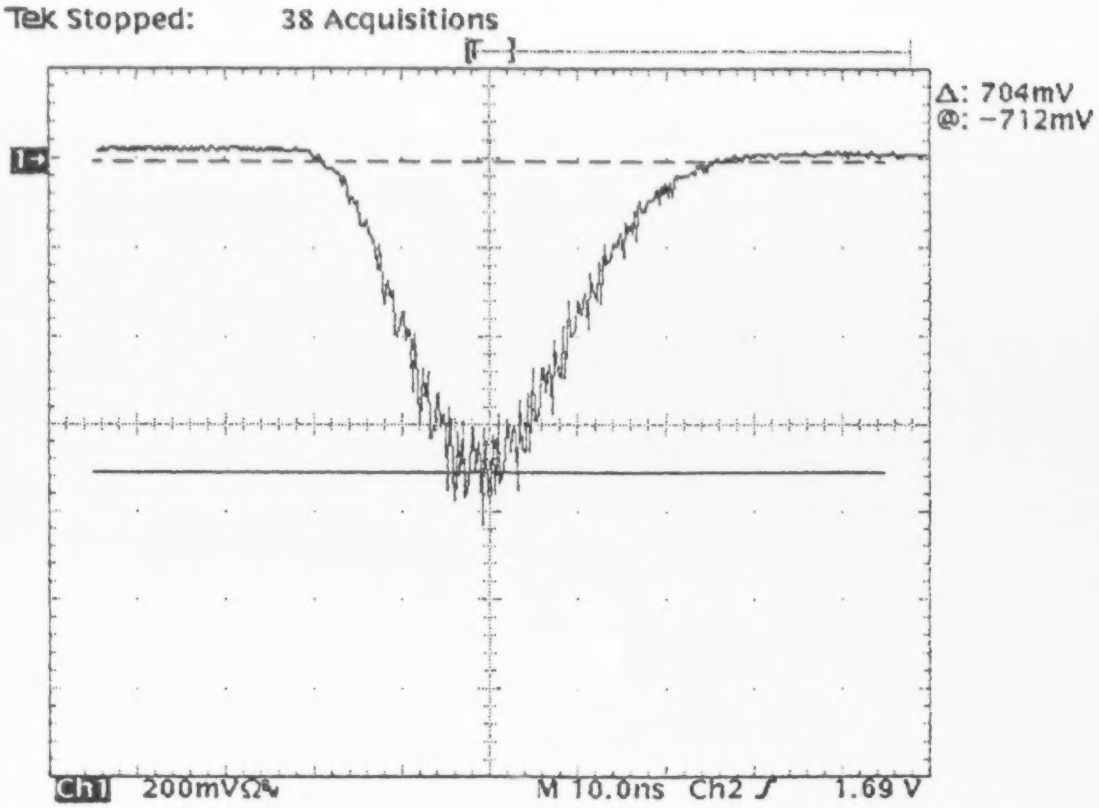

Figure 29 - Decay curve (w-7, room temperature)

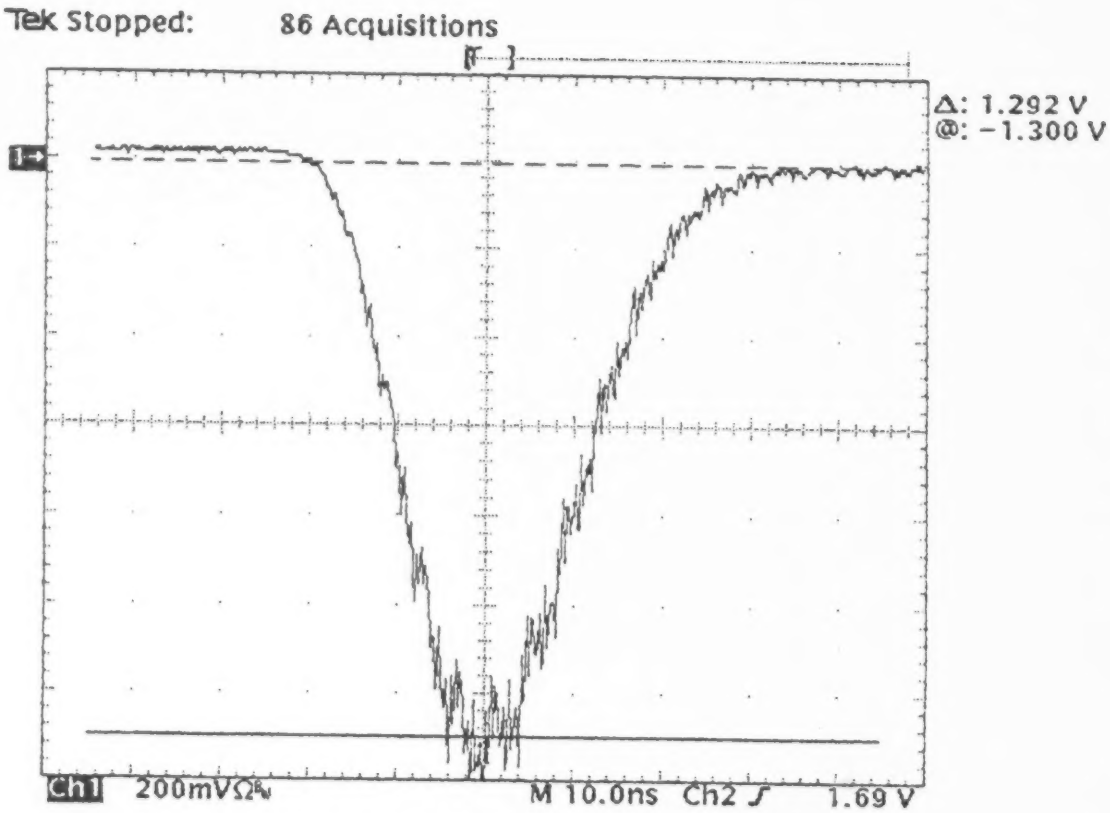

Figure 30 - Decay curve (w-7, liquid nitrogen temperature)

5. Summary AND DISCUSSION

Aspen is the major raw material for paper production in Canada. Its low lignin content and intrinsic whiteness make it an ideal wood if only it were consistently disease free. Unfortunately various forms of decay and stain create processing difficulties, and automated recognition and rejection techniques of seriously defective wood before pulping takes place would be advantageous.

A series of laboratory measurements were done on samples of clear and discolored aspen wood to find optical characteristics which, at some later stage, could be applied in industry to reject unsound wood. In addition to that, the study was expanded as a matter of general interest to transmission and luminescence measurements and theoretical calculations.

Three different optical properties of aspen wood were investigated. We measured reflection spectra, transmission spectra, and luminescence. Of these three, the reflection spectra appear to be the most applicable. It is found that the reflection intensities of clear wood samples are higher than that of darker samples confirming the reflection measurements of Klapstein, K. P., Weichman, F. L., Bauer, W. L., and Kenway, D. J. (1989) for other wood species. Although reflection intensities with respect to the clear aspen wood decrease with decreasing wave length, there is again an increase in the violet and near UV region with minima around λ = 450 nm. A significant difference in the reflection intensities can be seen for the sample which has black patches. Its reflection intensities increase with decreasing wavelength over the entire range as compared to the clear wood. In retrospect we should have examined more

samples from the wood with black patches to be able to classify the wood with black patches having consistently different characteristics from other parts of the wood. One general conclusion can definitely be drawn. The best wavelength region where the brown wood can be distinguished from clear wood by measuring reflection intensities with respect to the clear wood is the blue region in which clear wood has higher reflection intensities than brown wood by as much as 50%.

Transmission measurements show no promise in the field, they are however of interest in a more basic sense. We have measured transmission intensity ratios of light of different wood samples with respect to the thickness at different wavelengths and found significant differences between clear and defective specimens. Transmission intensities are higher for clear wood than for the defective wood. There is also a very significant difference between the transmission of light along and across the grain. Light travelling along the grain is attenuated much less than light travelling across the grain. Light travelling along the grain means light travels the length of the wood fibers while light travelling across the grain means light travels across the fibers; ie. across fiber walls. Since the part of light is reflected each time when light travels across the fiber walls, the transmission intensity of light travelling across the fibers is lower than light travelling along the fibers.

As a supplement to the experimental work, we have also done some computer modelling on an oversimplified wood-like structure to see if and how the concept

of an absorption constant makes sense in specifying the transmission characteristics of wood.

In our calculations of transmission, when the total relative transmission intensity was calculated, only the amplitude of the light waves has been considered. The intensity of the wave is directly dependent on not only the amplitude but also the phase. But in the case of real wood, since the surface is irregular, interference cannot be expected to be important. Therefore, the inclusion of the phase information is irrelevant.

When light travels through the wood fiber, some part of the light is absorbed by the wood due to its absorption coefficient. In the calculations, the loss of light which is absorbed by the fiber was not considered. Also only the case of E perpendicular to the plane of incidence ($E_{\perp}$) was considered in the calculations for simplicity. E parallel to the plane of incidence ($E_{//}$) should have been calculated separately. For the smaller angles of incidence with respect to the incident light, there is not much difference between amplitude coefficients of reflection and transmission for the two cases of $E_{\perp}$ and $E_{//}$. But, for higher incident angles, $E_{//}$ can't be neglected because the difference between amplitude coefficients of reflection and transmission for the two cases of $E_{\perp}$ and $E_{//}$ are considerably larger for larger angles. Figure 24 shows the calculated transmission intensities over a range of angles (-180) - 180 for $E_{\perp}$. Therefore, a difference can be expected in $E_{\perp}$ and $E_{//}$ for larger angles. However, in the calculation of the absorption coefficient, transmission intensities from only the middle portion of the graph; ie. small angles of incidence with respect to the fiber

structure, were considered. Therefore, no significant difference in absorption coefficient is to be expected had $E_{//}$ been included.

For the experimental value of absorption coefficient of 0.75 mm^{-1}, the calculated value for the thickness of a single fiber is 1.2 mm in our model, where the refractive index was taken as 1.5. The actual diameters of the fibers are in the range of 0.01 to 0.02 mm. If the value of absorption coefficient had been calculated using a more realistic value for the diameter of the fiber, we would predict absorption coefficient as 60 mm^{-1} for n=1.5 although the measured value is in the range of 0.5 to 1.5 mm^{-1}. In the calculations, only the incident light entering to the fiber as a parallel beam perpendicular to the axis of the fiber was considered but the other light coming from the adjacent fibers was not included. If the light coming from the adjacent fibers is also included in the calculations, it can be guessed that the light transmission intensity will somewhat higher. The more the transmission, the lesser the value of absorption coefficient we get. However, the discrepancy between measured and calculated absorption coefficient is too large to ignore.

We have repeated the transmissions calculations for n=1.1, and found that about 60% of the incident intensity comes out within 15° of the incident light direction instead of 40% for n=1.5. Since more light is transmitted, we get lower absorption coefficient than for n=1.5. To create a better match between theory and the experiment, the effective refractive index should be decreased even further. One way to reduce the effective refractive index, is by assuming that the fibers are immersed in water or a liquid of refractive index closer to the refractive

index of the fiber since the effective refractive index is the ratio of refractive index of fiber to that of the liquid . This also makes sense in reality because wood contains a large amount of water.

Abnormalities in wood complicates the structure of wood. Deviations from normal are not uncommon, because trees are living organisms and are subject to various influences through their span of life. Therefore, when reflection and transmissions measurements are made, these abnormalities can cause noticeable differences. For an example, if a knot is present inside of the sample of wood, the grain direction can be completely different than expected and also the reflection intensities may be noticeably decreased. Please note that in these studies, samples were carefully chosen to avoid such structural abnormalities.

The model constructed for the transmission calculations needs major modification to predict the reflection measurements for light travelling across the grain. In the transmission measurements, the incident light falls on the fiber making an angle 90° with the layer of fibers when light travels across the grain. But in the case of reflection measurements for light travelling across the grain, incident light falls on the fiber making an angle of 30° with the fiber layer. The reflection intensity at 90° direction with respect to the that incident direction can be calculated by the model for a single fiber. But, when we consider a layer of fibers, some incident light and some reflected light is blocked by the adjacent fibers when the incident angle is 30° with the fiber layer. Therefore, more time should have been spent to do a major modification to the model of transmission behavior to calculate the reflection characteristics.

In considering this model; however; it is important to emphasize the simplifying assumptions, especially that wood consist of a single cell type (referred as "fibers" and that transmission of light is similar through radial and tangential sections of wood.

Finally, luminescence measurements were made as a function of emission wavelength for different wood samples. It could be seen that all luminescence spectra for different samples with different diseases exhibit the same shapes with a common peak at 535 nm. Since it is known that the luminescence intensities are higher, show more structure and that the decay is usually slower at low temperatures, it was decided to check the luminescence intensity and decay time at 77°K (-192°C). This low temperature was chosen because it is the boiling point of liquid nitrogen and liquid nitrogen is readily available and easy to use. Although the decay times of the samples at room temperature and liquid nitrogen temperature were too short to be resolved, higher luminescence intensity was noticed at liquid nitrogen temperature. Luminescence, although found to be strongest in defective wood, is not localized in those parts of the tree which are of concern to the paper making process. It was noticed that luminescence does not only appear in the defective wood but also can be seen at the edges of the rotten parts and in some areas of white wood.

Bibliography

Airth, R. L. , Foerster, G. E. , and Behrens, P. Q. , The Luminous Fungi, **Bioluminescence in Progress** (1966), Proceedings of the luminescence conference (1965), Edited by Johnson F. H. , and Haneda Y. , Princeton University Press, New Jersey, P. 203-224

Breck, D. , Aspen Defects : Their Importance to Pulp and Paper, **Proceedings of aspen quality workshop** (1987), Forestry Canada, Northern Forestry Center, Alberta, P. 6-22

Defense Mechanics of Woody Plants Against Fungi, Edited by Blanchette, R. A. , and Biggs, A. R. , Springer-Verlag, Berlin (1992)

Derkson, W. L. and Monahan, T. I. , A Reflectometer for Measuring Diffuse Reflectance in the Visible and Infrared Regions, **J. Opt. Soc.** Am. 42, 263-000 (1952)

Desch, H. E. , **Timber : Its Structure and Properties**, Fifth Edition, The Macmillan Press Ltd. , London (1973)

Frei, R. W. and MacNeil, J. D. , **Diffuse Reflectance Spectroscopy in Environmental Problem Solving**, CRC Press, Cleveland (1973)

Harlow, W. E. , Hurrar, E. S. , White, F. M. , **Textbook of Dendrology**, McGraw-Hill Inc., New York (1979)

Haygreen, J. G. and Bowyer, J. L. , **Forest Products and Wood Science** (1982), The Iowa State University Press, Lowa, P. 45-61

Hecht, E. , **Optics**, Addison-Wesley Publishing Company, Inc. , California (1990)

Hiratsuka, Y. and Loman, A. A. , Decay of Aspen and Balsam Poplar in Alberta, **Information Report NOR-X-262**, Northern Forest Research Center, Canadian Forestry Service (1984)

Hiratsuka, Y. , Gibbard, D. A. , Bakowsky, O. , and Maier, G. B. , Classification and Measurement of Aspen Decay and Stain in Alberta, **Information Report NOR-X-314**, Forestry Canada, Northwest Region, Northern Forest Research Center (1990)

Klapstein, K. D. , Weichman, F. L. , Bauer W. L. , and Kenway, D. J. , Optical Characteristics of Wood Stain and Rot, **J. App. Optics** Vol. 28 No. 20, P. 4450-4452 (1989)

Kollman, F. P. , Kuenzi, E. D. , and Stamn, A. J. , **Principles of Wood Science and Technology**, Springer-Verlag, Berlin (1975)

Lindsay, J. P. , Gilbertson, R. L. , **Basidiomycetes That Decay Aspen in North America**, J. Cramer, Lehre, West Germany (1878)

Macleod, J. M. , Chemical Pulping of Aspen : Possibilities and Realties, **Proceedings of the workshop on aspen pulp, paper, and chemicals**, (1978), Edited by Wong, A. and Szabo, T. , Forestry Canada, Northern Forestry Center, Alberta, P. 25-41

Macleod, J. M. , Berlin, R. W. , Gooding, R. W. , and Cyr, N. , Upgrading Decayed Aspen, **Proceedings of the 1982 TAPPI conference**, Toronto, Ontario, P. 75

Mathews, P. C. and Beech, B. H. , Method and Apparatus for Detecting Defects, **United State Patent**, Patent Number 3,976,384 (1976)

Mathews, P. C. and Soest, J. F. , Method for Determining Localized Fiber Angle in a Three Dimensional Fibrous Material, **United State Patent**, Patent Number 4,606,645 (1986)

Nault, J. R. and Manville, J. F. , Differentiation of Some Canadian Coniferous Wood by Combined Diffuse and Specular Reflectance Fourier Transform Infrared Spectrometry, **J. Wood and Fiber Science** V. 24, P. 424-431 (1992)

Preliminary Assessment of Impulse Radar to Detect Decay in Hardwood (1987), Canpolar Inc. , Project No: 1043, Published by Canadian Forestry

Service, Northern Forestry Center, Alberta

Stamm, A. J. , **Wood and Cellulose Science**, The Ronald Press Company, New York (1964)

Thomas, G. P. , Etheridge, D. E. , and Paul, G. , Fungi and Decay in Aspen and Balsam Poplar in the Boreal Forest Region, Alberta, **Can. J. Bot.** 38 (1960) P. 459-466

Tsoumis, G. , **Science and Technology of Wood Structure, Properties, Utilization**, Van Nostrand Reinhold, New York (1991)

Wassink, E. C. , Luminescence in Fungi, **Bioluminescence in Action** (1978), Edited by Herring P. J. , Academic Press, London, P. 171-198

APPENDIX I

```
CLS
10  INPUT R
20  FOR X = .001 TO R STEP .001
30  A = (X/R)
40  B = SQR (1-A^2)
50  D = X / (1.3*R)
60  C= SQR (1 - D^2)
70  R(1 ) = ( B - (1.3*C ) ) / (B + (1.3*C ) )
80  R( 2 ) =  - R(1 )
90  t( 1 ) = 2 * B / ( (1.3*C ) + B )
100 t( 2 ) = 2*1.3*C / ( (1.3*C ) + B )
110 E = A / B  :  F = D / C
120 G = ATN(E) * 57.29578  :  H = ATN(F) * 57.29578
130 LPRINT "X="; X;  "& INCIDENT ANGLE="; G
140 LPRINT  2*G; TAB(15) ; R(1) ^2
150 LPRINT 180 + (2 *(G-H ) ) ; TAB(15) ;   ( (t(1) * t(2) ) ^2 ) * B
160 LPRINT 360 + (2*(G-2*H) );TAB(15) ; ((t(1)*t(2) *R(2) )^2 ) * B
170 LPRINT 180 + (2*(G-3*H)) ;TAB(15); ((t(1)*t(2)*(R(2))^2)^2 ) * B
180 LPRINT 360 + (2*(G-4*H)); TAB(15); ( (t(1)*t(2)*(R(2))^3)^2 ) * B
190 LPRINT
200 LPRINT "X="; -X;  "& INCIDENT ANGLE="; G
210 LPRINT (360 - 2*G); TAB(15); ( R(1) )^2
220 LPRINT 180 - 2*(G - H) ); TAB(15) ; ( (t(1)*t(2))^2) * B
230 LPRINT  -(2*(G - 2*H) ); TAB(15); ( (t(1)*t(2)*R(2) )^2) * B
240 LPRINT 180  -(2*(G - 3*H) );((t(1)*t(2)*(R(2))^2)^2 ) * B
250 LPRINT -( 2*( G - 4 *H) ); ( (t(1)*t(2)*(R(2))^3)^2 ) * B
260 LPRINT
270 NEXT X
280 END
```